A THEORY FOR THE GENERATION OF "INTERVALS OF PULSATIONS OF DIMINISHING PERIOD"

by

KENNETH R. ROXBURGH

B.Sc. (Hons), University of Alberta, 1966

A THESIS SUBMITTED IN PARTIAL FULFILMENT OF
THE REQUIREMENTS FOR THE DEGREE OF

DOCTOR OF PHILOSOPHY

in the Department

of

GEOPHYSICS

We accept this thesis as conforming to the
required standard

THE UNIVERSITY OF BRITISH COLUMBIA

August, 1970

Department of **Geophysics**

The University of British Columbia
Vancouver 8, Canada

Date **September 4, 1970**

ABSTRACT

Micropulsation data recorded at Palo Alto, California during 1963-4 and Ralston, Alberta during 1967 have been used to study "Intervals of pulsations of diminishing period" (IPDP). IPDP's are found to be generated in the dusk-midnight quadrant of the magnetosphere at an equatorial distance of about 6 earth radii. An intensive study of the Ralston data reveals that IPDP's occur during the expansive phase of magnetospheric substorms.

It is proposed that IPDP's are generated by a cyclotron instability between energetic protons and left-hand ion cyclotron waves. Their main characteristics are determined by the perturbations of the dusk-midnight sector of the magnetosphere by magnetospheric substorms. One of the main disturbances in that region is a slow decrease and then sudden increase in the magnetic field corresponding to the buildup and decay of a partial ring current. IPDP's show an increase in midfrequency due to the change in the cyclotron instability frequency produced by the increasing magnetic field. This theory is tested by a comparison of frequency increase of IPDP's observed at Ralston and magnetic field increase in the magnetosphere observed by the ATS-1 satellite.

Other conditions necessary for IPDP generation are then discussed. It is shown that different combinations of these conditions result in the generation of hm emissions and band type micropulsations.

TABLE OF CONTENTS

LIST OF FIGURES

LIST OF TABLES

ACKNOWLEDGEMENTS

I wish to thank Dr. T. Watanabe for his constant advice and encouragement and for many hours of discussion during the progress of this work. I am indebted to him for many criticisms and comments and for carefully reviewing the final manuscript.

Many persons have contributed in one way or another to this work. The Palo Alto micropulsation data were recorded by the Physics Research Laboratory of Lockheed Missiles and Space Company and I am indebted to all people involved in that operation. In particular I would like to thank Dr. A. C. Fraser-Smith now at Radioscience Laboratory, Stanford University for many suggestions and comments and for help in the reduction of Palo Alto data.

The ATS-1 magnetic data were made available through the co-operation of the Department of Planetary and Space Science, University of California, Los Angeles. I am indebted in particular to the people who did the reduction of satellite data to the form of magnetic field plots. I wish to thank Dr. R. L. McPherron for helpful discussions on the ATS-1 data and proposed IPDP generation theory.

I also thank my wife, Marja, for her patience over the last few years and for carefully reviewing the final manuscript.

This study was partially supported by a National Research Council of Canada research grant to Dr. T. Watanabe. The author gratefully acknowledges financial assistance in the form of an International Nickel Company of Canada Fellowship for one year, and a National Research Council Scholarship for three years.

CHAPTER I

Introduction

Early researchers in the field of geomagnetic micropulsations generated many different names for the diverse and complicated phenomena observed. In 1964 the nomenclature was simplified by reclassification of all micropulsations into two groups (Jacobs et al. 1964). Micropulsations with a continuous waveform were denoted by Pc , while irregular impulsive waveform micropulsations were denoted by Pi . Each group was subdivided on the basis of frequency (see Table I.1), but the division was based on the major morphological properties of the micropulsations.

Table I.1

Classification of Micropulsations

Type	Range of Periods (sec)
Continuous Pulsations	
Pc 1	0.2 - 5
Pc 2	5 - 10
Pc 3	10 - 45
Pc 4	45 - 150
Pc 5	150 - 600
Irregular Pulsations	
Pi 1	1 - 40
Pi 2	40 - 150

It is now known that some of the subgroups (namely Pc 1, Pi 1) contain several morphologically distinct micropulsations. Figure 1 is the sonagram representation, which displays frequency as the ordinate, time as the abscissa, and amplitude as the darkness, of a typical Pc 1 event. Such micropulsation signals displaying a regular repetition of rising tones have been called hydromagnetic (hm) emissions (Tepley and Wentworth, 1962), hm whistlers (Obayashi, 1964, Jacobs and Watanabe 1964b) and micropulsation whistlers (Jacobs and Watanabe 1964a). Jacobs and Watanabe (1967) argue, however, for the existence of at least two prototypes. One type displays the regular dispersion effects of an ion cyclotron mode wave (left-hand polarization) bouncing between a pair of magnetically conjugate areas under the guidance of the magnetic line of force and is thus named hm whistlers by Jacobs and Watanabe. The other type of Pc 1 signal is called periodic hm emission after its similarity to periodic VLF emissions. The structural elements of these signals do not show any regular dispersion.

Short intervals of pulsations (SIP), (Troitskaya 1961) Pi (c) events (Heacock 1967b), and 4-sec. period micropulsations (Heacock 1966) are examples of morphologically distinct Pi 1 micropulsations. SIP or Pi bursts (Heacock 1967b) are impulsive broadband events of short duration occurring near local midnight. Pi (c) events are observed in the midnight-dawn quadrant and have a more continuous, nonimpulsive character.

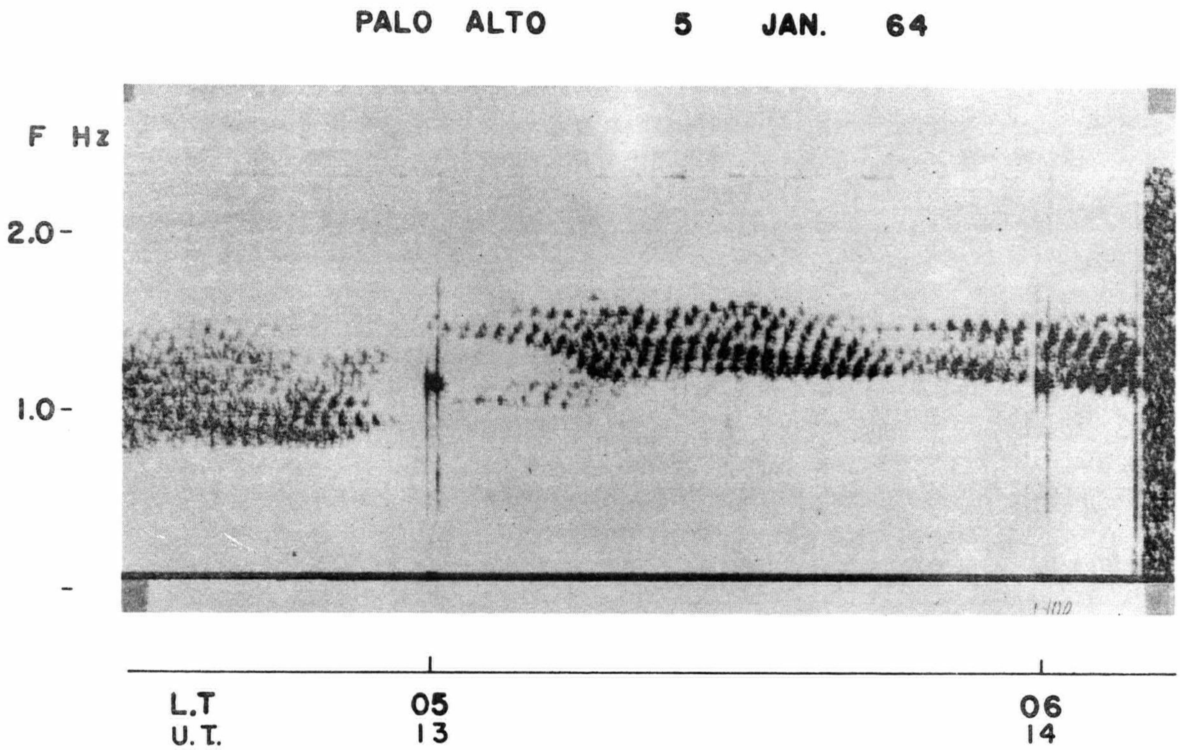

Fig. 1. Typical Pc 1 micropulsation

Figure 2a is a sonagram of a Pi burst at about 0200 local time (L.T.) followed by a Pi (c) event of about three hours duration. A 4-sec. period micropulsation has a constant frequency noise band character as illustrated in Fig. 2b, and is observed most often in the afternoon L.T. (Heacock 1966).

Intervals of pulsations of diminishing period, hereafter called IPDP, were first extensively studied by Troitskaya (1961). They have also been studied under the name of solar whistles (Duffus et al. 1959), gurglers (Tepley and Amundsen 1964, Tepley 1966) and sweepers (Heacock 1967a, Fukunishi 1969). IPDP's may have the waveform characteristics of either Pc 1 or Pi 1 micropulsation groups. In the sonagram representation, they consist of a diffuse noise band on which irregularly spaced structural elements are sometimes superimposed. Both the noise band and structural elements display a rise in midfrequency during the event which lasts from 10 to 45 minutes. The Pc or Pi waveform character is determined by the amount of noise, and irregularity of structure. Figure 3 is an IPDP shown in shaded and contoured sonagrams (see Chapter II for details). It has many structural elements as seen in the shaded sonagram, but they occur in three major groups as indicated in the contoured sonagram. The waveform of the IPDP shown in Fig. 3 resembles Pc 1 waveform. When the noise band dominates over the structure the IPDP waveform becomes irregular.

a)

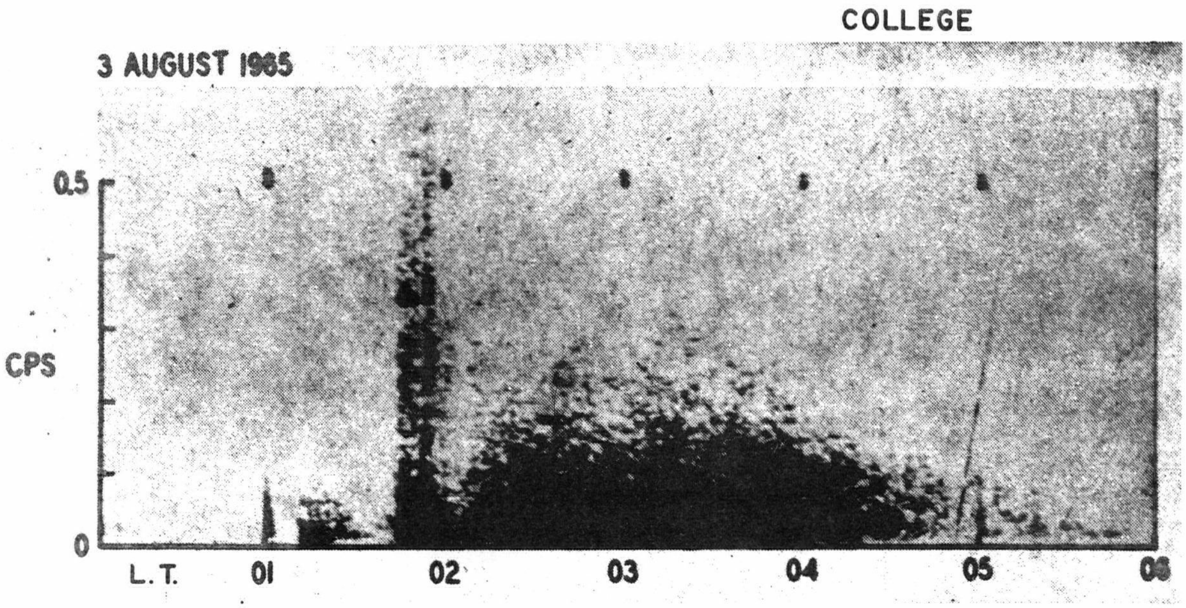

b)

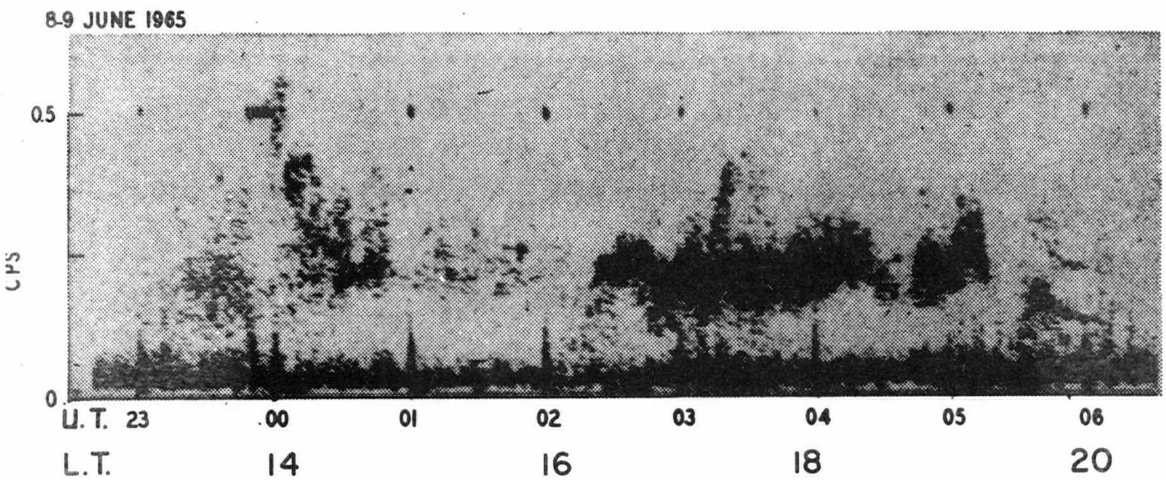

Fig. 2. Pi 1 type micropulsations

a) Pi burst followed by Pi(c) event (after Heacock 1967b)

b) 4-sec. period micropulsation (after Heacock 1966)

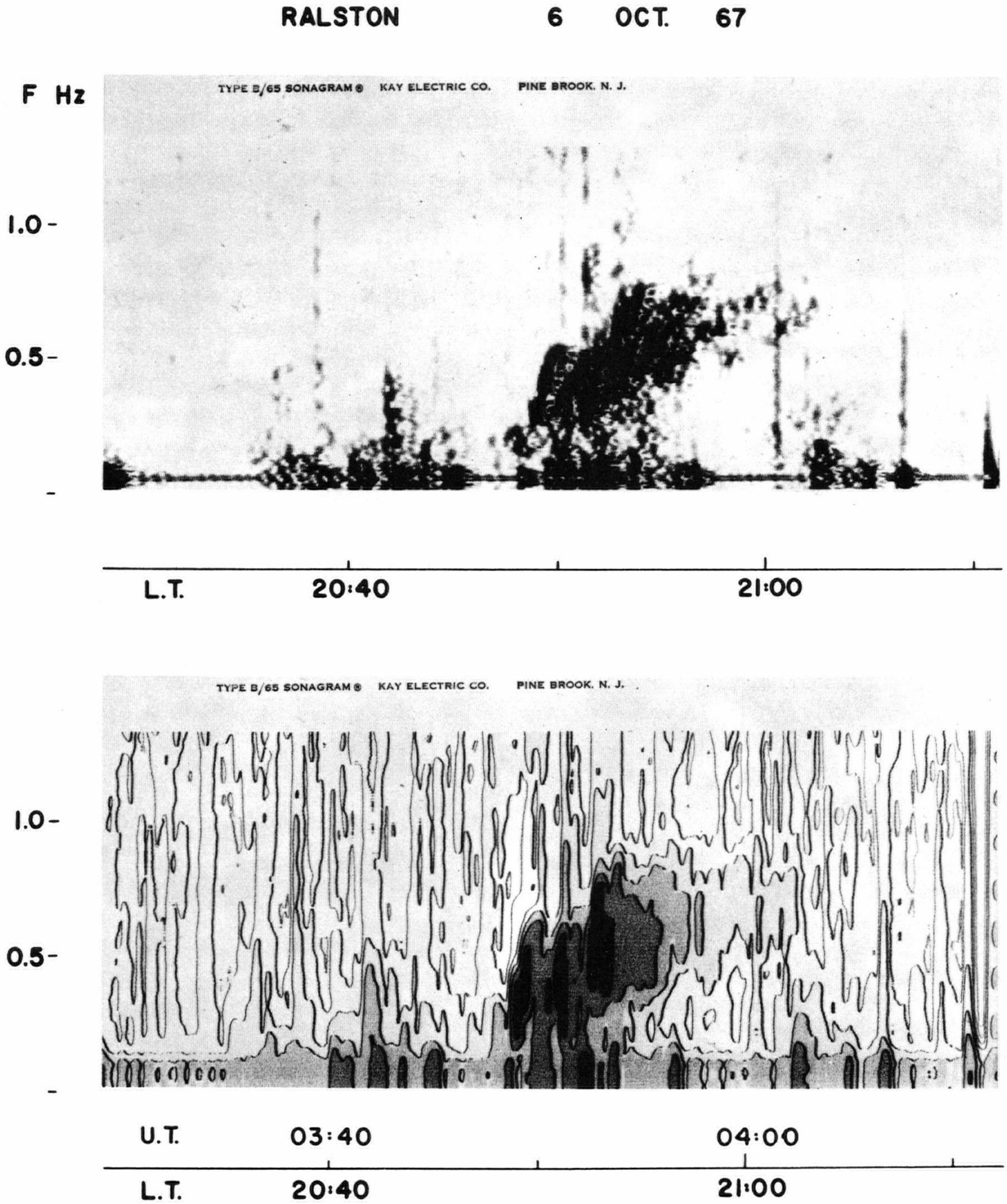

Fig. 3. Typical Ralston IPDP

The occurrence of IPDP's is related to the occurrence of other micropulsations and geomagnetic phenomena. Heacock (1967) has noted that a 4-sec. micropulsation band sometimes terminates in an IPDP. Gendrin et al. (1967) have observed the occurrence of hm emissions directly following an IPDP. It is thus likely that the generation processes for these three types of micropulsations have some common connection.

IPDP's also occur in conjunction with magnetospheric substorms (Troitskaya 1961 and others). A knowledge of IPDP characteristics and generation mechanism will be very useful in furthering the understanding of the magnetospheric substorm process. This thesis will show that IPDP's are produced by a specific combination of conditions existing in the dusk-midnight quadrant of the magnetosphere during magnetospheric substorms. Different combinations of these conditions will be shown to lead to other Pc 1 frequency micropulsations.

The magnetospheric substorm process is reviewed in Chapter III. Chapter IV presents the experimental data and develops the IPDP generation mechanism. Chapter V is a discussion of the proposed and other IPDP theories. There the relationship of IPDP's, hm emissions, and band type micropulsations will also be discussed.

CHAPTER II

Data Sources, Analysis and Instrumentation

II.1 Micropulsation Data Source and Instrumentation

Micropulsation data from two separate research projects have been used in this thesis. The Ralston 1967 data were recorded through a cooperative field operation by Radio Science Laboratory, Stanford University, the Pacific Naval Laboratory (now D.R.E.P.), and the University of British Columbia. The Physics Research Laboratory of Lockheed Missiles and Space Company recorded the Palo Alto 1963-64 micropulsation data. Table II.1 gives the location of both recording stations.

Table II.1
Location of Micropulsation Stations

Station	Geographic		Geomagnetic	
	Lat. (N)	Long. (W)	Lat. (N)	Long. (E)
Ralston	51°12'	111°07'	58.8°	305.5°
Palo Alto	37°26'	122°10'	43.5°	299.0°

The Ralston micropulsation detection system consisted of mumetal cored solenoids in the geographic north-south (X), east-west (Y), and in the vertical (Z) directions. The signals from these coils were fed through dc chopper amplifiers to a slow speed FM recording system using a carrier of 22.5 hertz and having a band pass of 0 to 4 hertz. The tape speed for recording was 0.025 inches per second whereas the reproduction speed is 3.75 inches per second, giving a frequency multiplication of 150. At these speeds, 10 days of data recorded on 1800 feet of tape can be played back in 1.6 hours.

Channels 1, 2, and 3 of the magnetic tapes contain the X, Y, and Z micropulsation components. Also, minute and hour marks were multiplexed on channels 1 and 2 respectively and are available as separate outputs on reproduction. Frequency calibration was achieved by periodically recording a calibration tone consisting of frequencies in steps from 0.03 to 6.0 hertz. A simultaneous recording of the Y component was made on a Helicorder chart operating at 3 cm. per minute. Weir (1966) and Gibb (1968) give a complete description of the micropulsation recording system.

The Palo Alto micropulsation system uses mumetal cored solenoids in the X and Y directions. The coil signals are fed to the recording system through galvanometer photo-tube amplifiers. The signals which are then in the 0.02 to 7 hertz band are recorded on an AM tape system running at 0.03 inches per second by amplitude modulating a 1000 hertz bias signal. Both channels are also recorded on Helicorder charts operating at 6 cm. per minute. Time and frequency calibration are achieved by recording a two-minute tone of known frequency at the beginning of every hour. Tepley (1961, 1962) fully describes the instrumentation at the Palo Alto station. The data made available to this author was rerecorded on AM tapes which, when played at

3.75 inches per second, had a frequency multiplication of 2000.

II.2 Magnetic Field Data

Magnetograms from the ATS-1 satellite were made available through the cooperation of the Department of Planetary and Space Science, University of California, Los Angeles.

The ATS-1 satellite is in a synchronous equatorial orbit at 151°W and 6.6 Re geocentric distance. The magnetometer experiment consists of two orthogonal flux gates, coplanar with satellite spin axis, but with their sensing axes inclined 45° to the spin axis.

The magnetic fields perpendicular and parallel to the spin axes are determined by taking the sum and difference of the outputs of the two detectors. The magnetic field is then converted into H, D, and Z components as for an earth based magnetic observatory - H is positive northward, D positive eastward, and Z positive outward. The relative accuracy of individual measurements is $\pm 0.1\ \gamma$ but the absolute value of D and Z is $\pm 1\ \gamma$ and H is $\pm 10\ \gamma$ (Cummings et al. 1968). For a complete description of the satellite experiment see Barry and Snare (1966). (See Appendix IV for explanation of magnetic components.)

All the data analysis has been done by the U.C.L.A. group. The data were made available in the form of 15 sec. and 6 min. average plots of the H, D, and Z components.

Magnetograms from World Data Center observatories have also been extensively used for the research presented in this thesis. Table II.2 is a list of the magnetic observatories used with their geographic and geomagnetic co-ordinates.

II.3 Analysis of Micropulsation Data

A spectral representation or sonagram is the most useful form for micropulsation data. A sonagram displays frequency as the ordinate, time as the abscissa and amplitude as the darkness of shading. The Helicorder charts are used only to locate the micropulsation event and for a quantitative measure of its magnitude. Time and frequency measurements are made directly from the sonagrams. The initial data analysis therefore consists of the production of suitable sonagrams for all the events being studied.

For the Ralston data, the channel to be analysed (X, Y or Z) is combined with the hour marks through a resistor network and then fed into a Kay Electric 7030 A sonagraph (see Appendix I for specifications). Later in the research a second channel was added to the sonagraph. Then the time signal was recorded separately on this channel and displayed at the bottom of the sonagram.

Table II.2

Location and Magnetic Elements of Magnetic Observatories

Station		Geographic Co-ordinates		Geomagnetic Co-ordinates		Average Total Field (γ)		
		Lat. (N)	Long. (W)	Lat. (N)	Long. (E)	X	Y	Z
Ft. Churchill	(CH)	58°48'	94°06'	68.8°	322.5°	6,857	409	60,692
Baker Lake	(BL)	64°18'	96°23'	73.9°	314.8°	4,059	253	60,389
						H	D	Z
Leirvogur	(LEI)	64°11'	21°42'	70.1°	70.2°	11,688	336°19'	49,348
Great Whale River	(GW)	55°16'	77°47'	66.8°	342.2°	9,450	338°21'	58,700
Meanook	(MEA)	54°37'	169°50'	61.8°	301.0°	12,500	23°31'	57,700
College	(COL)	64°52'	147°50'	64.6°	256.5°	12,610	28°07'	55,227
Sitka	(SIT)	57°04'	135°20'	60.0°	275.3°	15,418	28°09'	54,712
Barrow	(BA)	71°18'	156°45'	68.5°	241.1°	8,850	22°40'	56,050
Victoria	(VIC)	48°31'	123°25'	54.3°	292.7°	18,803	22°11'	53,090
Boulder	(BOU)	40°08'	105°14'	49.0°	316.5°	21,135	13°43'	51,805
Fredericksburg	(FRED)	38°12'	77°22'	49.6°	349.8°	19,367	6°59'	52,808
Dallas	(DA)	32°49'	96°45'	43.0°	327.7°	24,282	8°39'	47,415
Tuscon	(TU)	32°15'	110°50'	40.4°	312.2°	25,785	12°58'	43,615

The sonagraph analyses the signal by first recording it on the edge of a turntable which is directly connected to the drum on which the sonagram is produced. This arrangement provides automatic time synchronization. The sonagram frequency is calibrated by recording a short interval of a 50 hertz signal along with its harmonics. In the reproduce mode the sonagraph turntable rotates at a speed such that the recorded signal varies from 0.96 to 96 KHz. The sonagram is traced by a stylus which advances upward on the reproduce drum, at the same time changing an oscillator frequency from 200 to 296 KHz. This variable carrier frequency is mixed with the recorded signal producing frequencies which are the sum and difference of the two signals. The modulator output is filtered by a band pass filter set at 200 KHz. This process of mixing and filtering enables the sonagraph to scan the recorded signal.

Two types of amplitude displays are available. The conventional display indicates the amplitude by the relative darkness of the sonagram. The recording paper has a dynamic range of 10 db but 40 db signals may be compressed on it by use of an AGC circuit. The second display contours the amplitude of the frequency time plots in steps of 6 db with a dynamic range of 42 db. The contoured intervals are also relatively shaded for ease of identification.

The Palo Alto micropulsation tapes were analysed on a Kay Electric Missilizer which is very similar to a Kay Electric

7030 A Sonagraph. However, a contour display is not available with this machine. The anlysis procedure was much the same as for Ralston data. The tapes had an hour mark at a known frequency, however, providing automatic time and frequency calibration of the sonagrams.

CHAPTER III

Review of Polar Magnetic Substorms

III.1 Introduction

In order to better understand the implications of some of the data to be presented in Chapter IV, a very short review of polar magnetic substorms will be given here. This review is in no way intended to be comprehensive but will concentrate on the gross spatial and temporal variations of substorm associated magnetic field changes.

A magnetospheric substorm is an explosive process occurring throughout the magnetosphere and ionosphere, lasting from 1 to 3 hours. It is an integral part of a magnetospheric storm, but also occurs during more magnetically quiet periods. Akasofu (1968) divides the magnetospheric substorm as manifested in the polar upper atmosphere into seven parts - auroral, polar magnetic, ionospheric, X-ray, proton aurora, VLF emission, and micropulsation substorms. In the magnetosphere, substorms are manifested by magnetic disturbances and proton and electron flux variations. Each substorm component has its own spatial and temporal characteristics and at present the relationship between them is not adequately understood. In this chapter, only polar magnetic substorms and associated magnetic disturbances in the magnetosphere will be reviewed.

III.2 Polar Magnetic Substorms

A typical magnetic disturbance at the earth's surface during a magnetospheric substorm is a sudden deviation from the normal baseline lasting up to three hours (magnetic bay). The magnitude, direction, and form of the bay depend on the latitude and local time of the observatory as well as the temporal characteristics of the substorm.

The gross spatial variation of magnetic bays is well illustrated by the substorm on October 6, 1967 (Fig. 4). The magnetic disturbance, starting at about 03:30 U.T., is large and complex near the auroral zone (GW, CH, MEA, COL). The maximum disturbance occurs near local midnight (GW, CH). Midlatitude stations (BOU, VIC) observe smaller magnitude bays with usually a simple form. Also both positive and negative bays are observed simultaneously at different observatories (MEA, VIC, COL).

It is customary to represent a polar magnetic substorm by a current system located in the ionosphere. The original current configuration (Silsbee and Vestine 1942) was based on the average of many bays and tended to point to the existence of two auroral electrojects, one flowing eastward before midnight and one flowing westward after midnight (Fig. 5a). More recently, Akasofu et al. (1965b, 1966a) and Feldstein (1966) have found that the jet current flows continuously westward along the

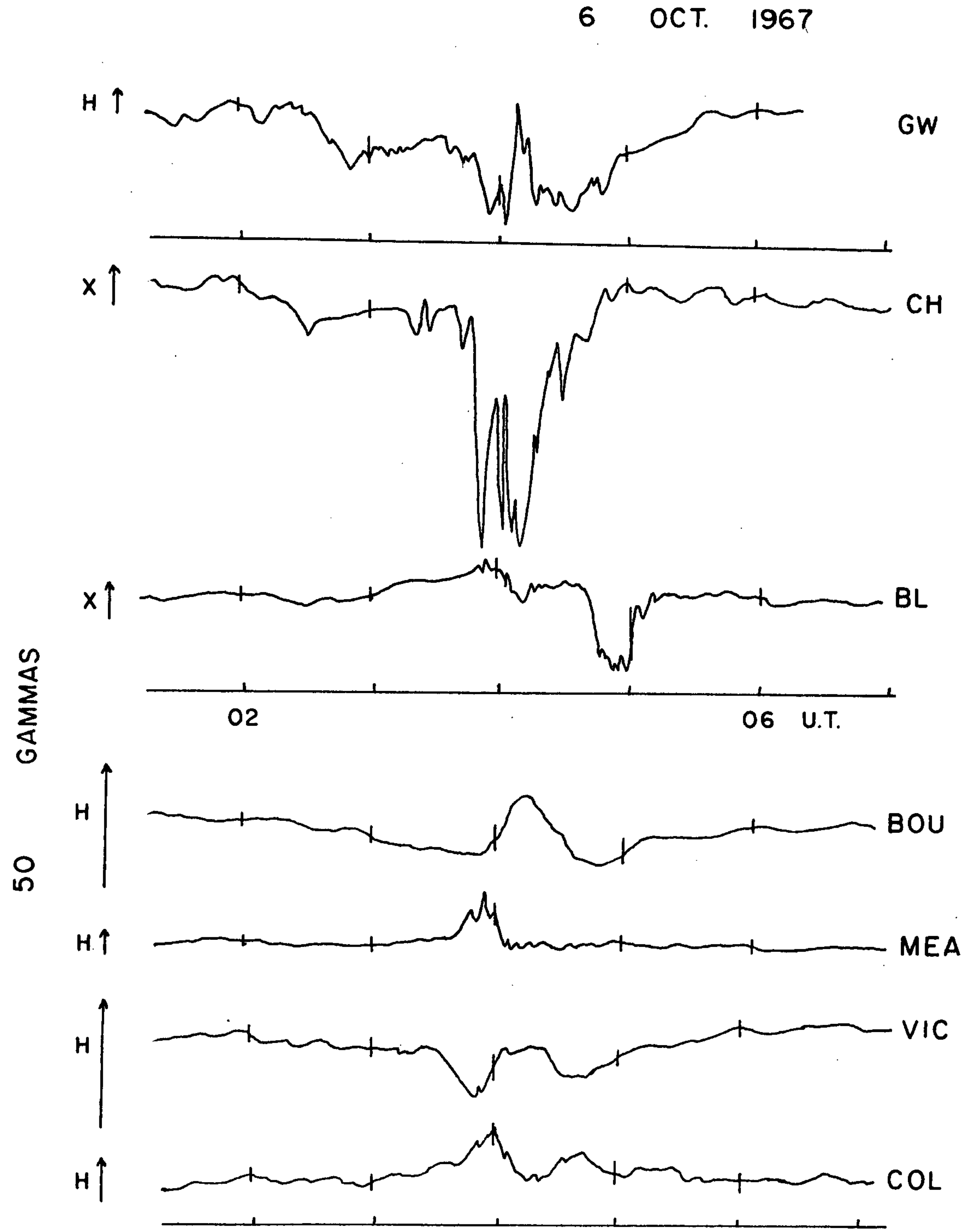

Fig. 4. Magnetograms showing the spatial variation of magnetic bays

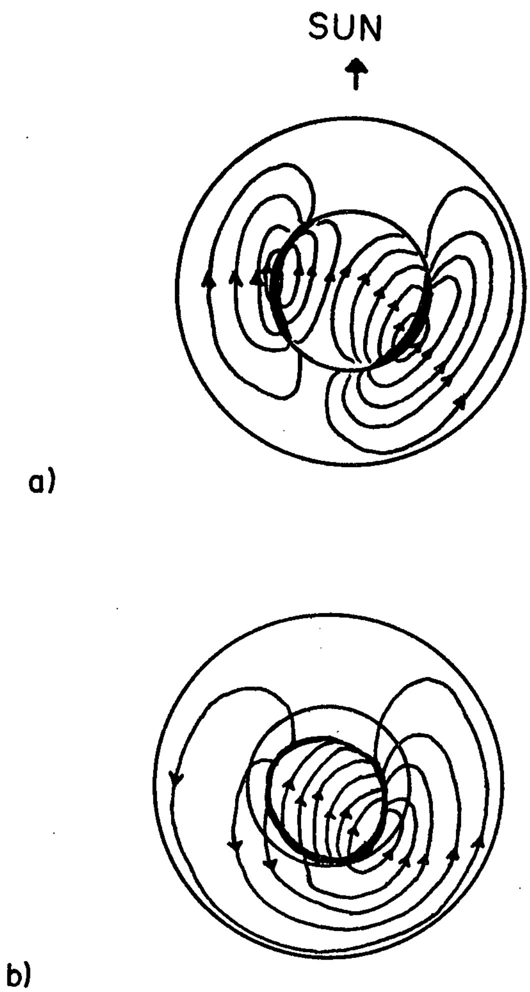

Fig. 5. Polar magnetic substorm equivalent current systems with

a) two cells

b) one cell (after Akasofu et al. 1965b) auroral oval (Fig. 5b). In both models the return currents are of much lower surface density than the primary electrojets. A detailed study by Best et al. (1968) shows that both types of current systems may occur during the same disturbed period but in different phases of it. Thus the temporal behaviour of magnetospheric substorms changes the form as well as the magnitude of the current systems.

Recently it has been shown that field aligned currents are also important in the production of magnetic disturbances (Zmuda et al. 1966, Atkinson 1967, Cummings et al. 1968). Cummings et al. (1968) showed that substorm magnetic field changes in the dusk-midnight quadrant at ATS-1 (6.6 Re) and Honolulu were in the same direction and of comparable magnitude. The field changes must thus be of magnetospheric origin as ionospheric currents would produce magnetic fields of opposite sign. Also Atkinson (1967) has been able to explain complicated magnetic disturbances near the auroral bulge by the use of field aligned currents.

The existence of magnetospheric currents means that a three dimensional current system must be used to explain substorm associated magnetic field changes. The current systems sketched in Fig. 5 must be considered to be equivalent current systems i.e. they symbolize the substorm magnetic disturbance by assuming that the causative current is flowing in the ionosphere.

Two contradictory 3-dimensional current systems have been proposed for polar magnetic substorms. Cummings et al. (1968) used ATS-1 magnetic field data to deduce the existence of a partial ring current in the dusk-midnight quadrant of the magnetosphere at a distance greater than 6.6 Re (Fig. 6a). The ring current is completed by currents flowing along the field lines into the ionosphere at about 1800 L.T. and out of the ionosphere at 2400 L.T. It would exist in addition to ionospheric currents with the general form of Fig. 5. Meng and Akasofu (1969) used ground magnetic data to deduce a partial ring current with a gap near local midnight (Fig. 6b). This model is not consistent with ATS-1 magnetic field measurements, which do not indicate a ring current on the day side of the magnetosphere. For this reason, Cummings' et al. model for substorm magnetospheric currents will be used in this thesis.

The exact nature of the temporal changes in the magnitude and form of current systems is unknown. However, magnetic disturbances in the auroral zone near local midnight are closely associated with auroral activity, namely the formation and motion of the auroral bulge and westward travelling surge (Akasofu et al. 1966a, b). At the time of auroral substorm expansive phase the currents which are flowing along the direction of auroral arcs (Sobuti 1961, Feldstein 1964 and others) are suddenly enhanced. The electrojet current then moves poleward with the expanding auroral bulge. The sudden and large

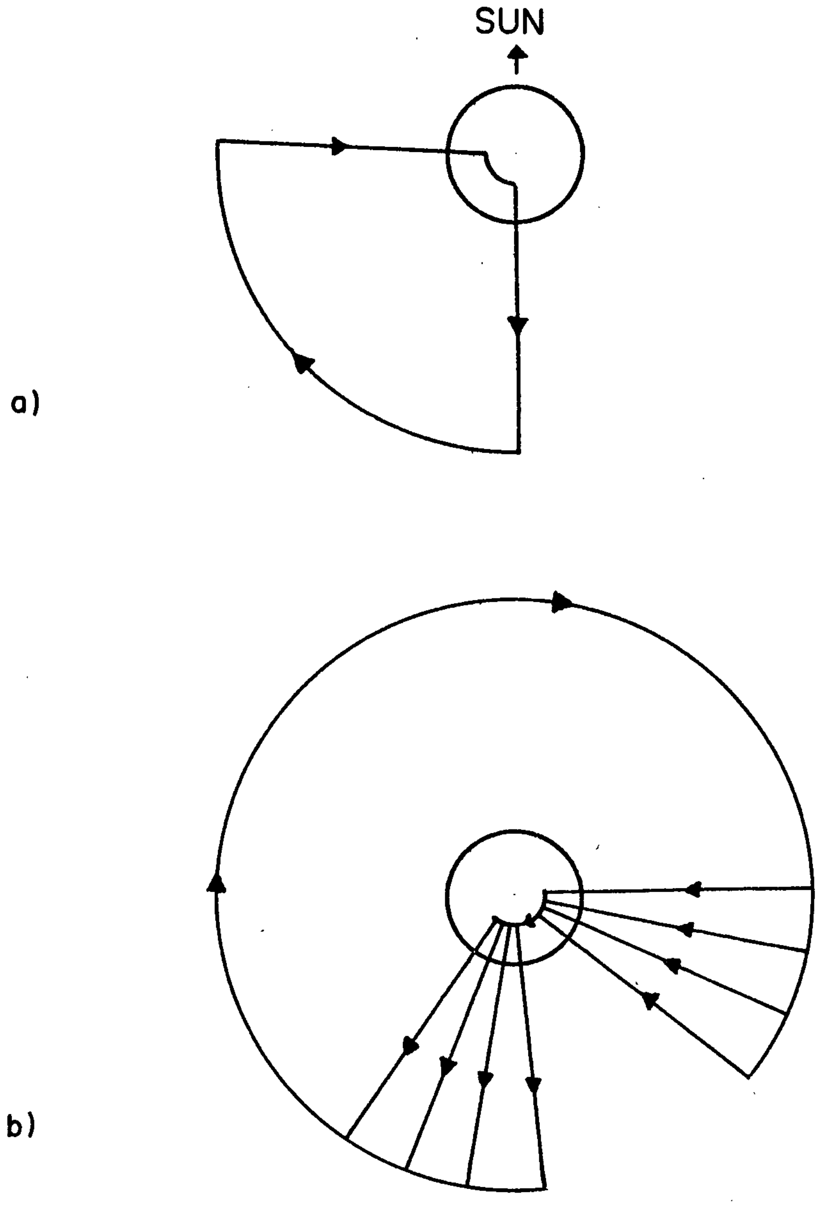

Fig. 6. An equatorial plane view from above the north geomagnetic pole of 3-dimensional current systems thought to be responsible for polar magnetic substorms (after a) Cummings et al. 1968, and b) Akasofu and Meng 1969)

magnetic disturbances seen in the vicinity of this moving electrojet can be used to identify the substorm expansive phase. Ideally one auroral zone observatory near local midnight is sufficient for this purpose, but practically a network of auroral zone observatories must be used since many substorms do not conform to the average substorm discussed above. Some substorms have localized magnetic field disturbances as will be shown in Chapter IV. Also the latitude range over which the electrojet moves during substorm expansion depends on the intensity of the substorm (Akasofu et al. 1966b).

The substorm temporal changes in the dusk region of the auroral zone are dominated by the passage of the westward travelling surge. (Akasofu et al. 1965a, Akasofu and Meng 1967). The magnetic disturbance in the dawn region is much less complex than that in either the dusk or midnight regions. It is dominated by the growth and decay, rather than the motion, of the current system.

Major magnetic disturbances occur during the substorm expansive phase, but there is evidence of significant magnetic activity previous to expansion. Rostoker (1968) has shown that the major excursion of the bay is often preceded by a smaller excursion having a duration of less than 20 minutes. Thus he argues that substorms occur in two stages, the second usually corresponding to auroral substorm expansive phase.

Cummings et al. (1968) noticed that when ATS-1 is in the dusk-midnight quadrant, the magnetic field slowly decreases, corresponding to the buildup of a partial ring current. At the time of, or shortly after the start of auroral substorm expansion, the field recovers to its pre-substorm value. The behaviour of the field at ATS-1 is illustrated in the magnetograms shown in Fig. 7. For both substorms occurring on May 11 the field at ATS-1 decreases previous to the time of substorm expansion as defined by the sudden changes at Great Whale. Polar magnetic substorms then consist of three phases - the quiet or buildup phase, the expansive phase and the recovery phase. The times of the expansive and recovery phases correspond to the times of the same phases for the auroral substorm.

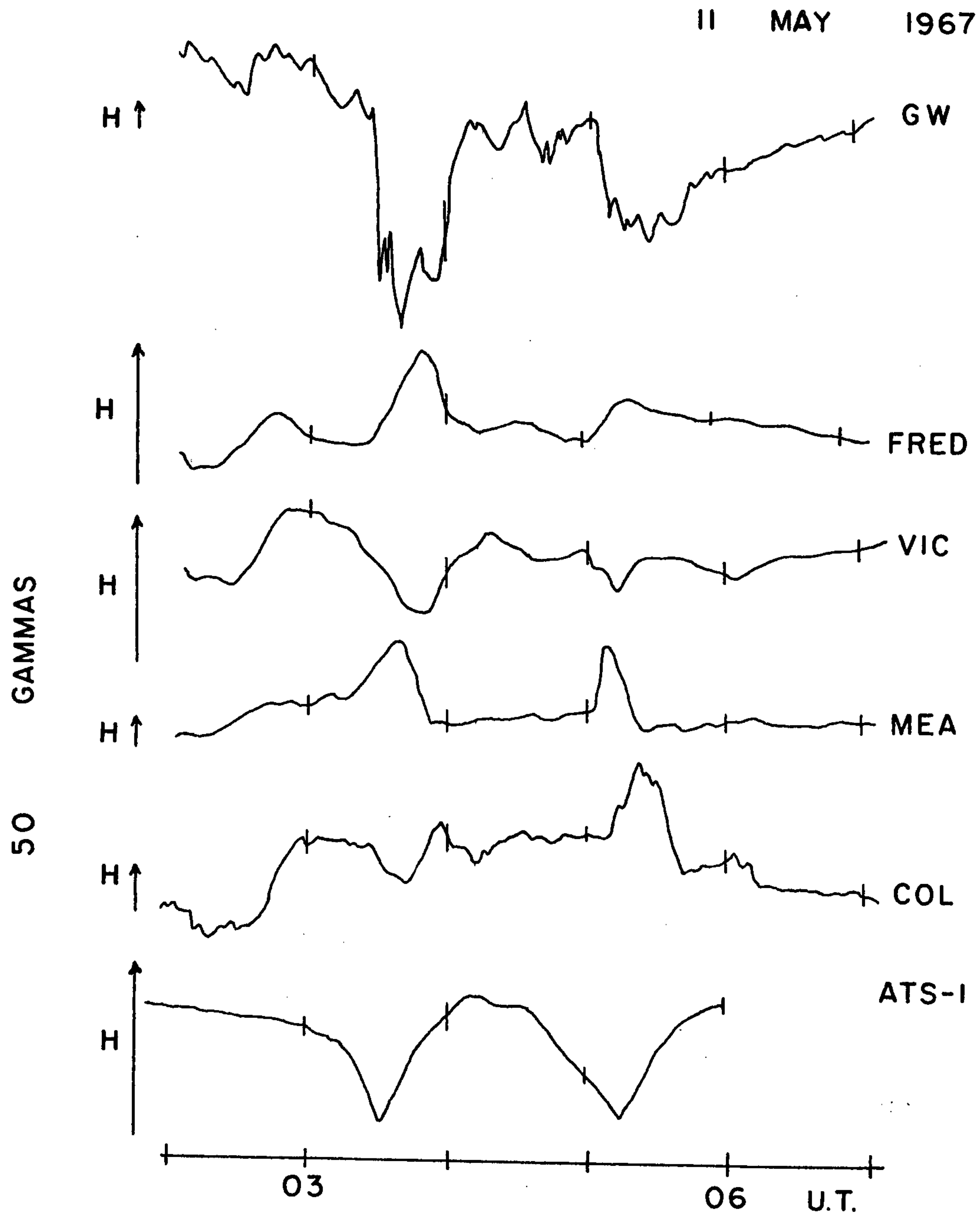

Fig. 7. Magnetograms showing the behavior of magnetic field at ATS-1 during polar magnetic substorms

CHAPTER IV

Properties of IPDP's

IV.1 Selection of IPDP Events

A continuous chart or magnetic tape recording of geomagnetic micropulsations may include many physically and morphologically different types. Therefore, in order to study a particular type of micropulsation such as IPDP, it must first be identified and separated from all other micropulsations. This identification is based on the distinct morphological properties of the micropulsation as observed in either the amplitude-time (paper chart) or frequency-time-amplitude (sonagram) displays. Different researchers may use a different selection process, thereby possibly influencing the final results. Because of this possibility, the process of IPDP selection for this thesis will be described in detail.

Troitskaya (1961) used the term "Irregular pulsations of diminishing periods" to classify a group of micropulsations whose frequency increased from approximately 0.1 to 1.0 hertz during its continuance of about thirty minutes. Further work by Gendrin et al. (1967), Heacock (1967a), and others revealed that the amount of frequency change is quite variable and that irregularly spaced structural elements are sometimes superimposed on the rising frequency noise band.

Heacock (1966) also observed so-called 4-sec. period micropulsations which sometimes appear very similar to IPDP's but have a constant frequency. Short intervals of pulsations, (S.I.P.), (Troitskaya 1961), are an example of pulsations having an infinite rate of frequency increase; i.e., they are an impulsive event with all frequencies observed simultaneously. Since the variation of the frequency increase of IPDP's extends almost to the extreme cases of 4-sec. pulsations and S.I.P., one must realize that the division becomes difficult.

Helicorder charts as described in Chapter II were searched for events in the 0.1 to 1.0 hertz frequency range whose average frequency increased with time. All these events were put into sonagram form and the IPDP sample was selected by elimination of events that: 1) had no measurable frequency increase and thus were probably 4-sec. period type micropulsations, 2) more closely resembled SIP or Pi(c) (Heacock 1967b), 3) were clearly recognizable as hydromagnetic emissions (Tepley 1962) by their regular repetition of rising structural elements. In cases (2) and (3) the frequency increase though observed on paper charts was due to the complex frequency-time structure of the emission.

An analysis of Palo Alto data for 1963-4 produced 35 IPDP's, 10 of which were too complicated to yield any meaningful frequency measurements. Ralston data for 1967 produced 39 IPDP's, of which 16 had a very complicated form.

IV.2 Characteristics of IPDP's

The characteristics of IPDP's are best observed in the spectrogram representation. Fig. 8 and 9 are examples of two quite different IPDP's shown in both shaded and contoured sonagrams. One can easily see the frequency increase of the broad-band noise in this representation. Structural elements superimposed on this noise band vary in number and form as shown by Fig. 8 and 9. Unlike hydromagnetic emissions, also known as hydromagnetic whistlers, or micropulsation whistlers, the structural elements do not have a simple repetitive period.

The duration of an IPDP is typically 20 to 30 minutes but some have been found to last only 10 minutes. Events lasting less than 10 minutes would not likely be classified as IPDP's because of the lack of an identifiable frequency increase; but they may be related in origin. When two rising frequency events were observed in one continuous micropulsation emission, they were classified as separate IPDP's. Their starting times were selected, as in the case of all IPDP's, at the beginning of the rising frequency segments.

Fig. 8 and 9 also illustrate the variability of the minimum, maximum, and midfrequency of IPDP noise band. For Ralston IPDP's, the minimum frequency varied from a low value to 0.3 hertz. The maximum frequency varied from about 0.6 hertz to above 1.0 hertz. Often there is no sharp cut-off in either

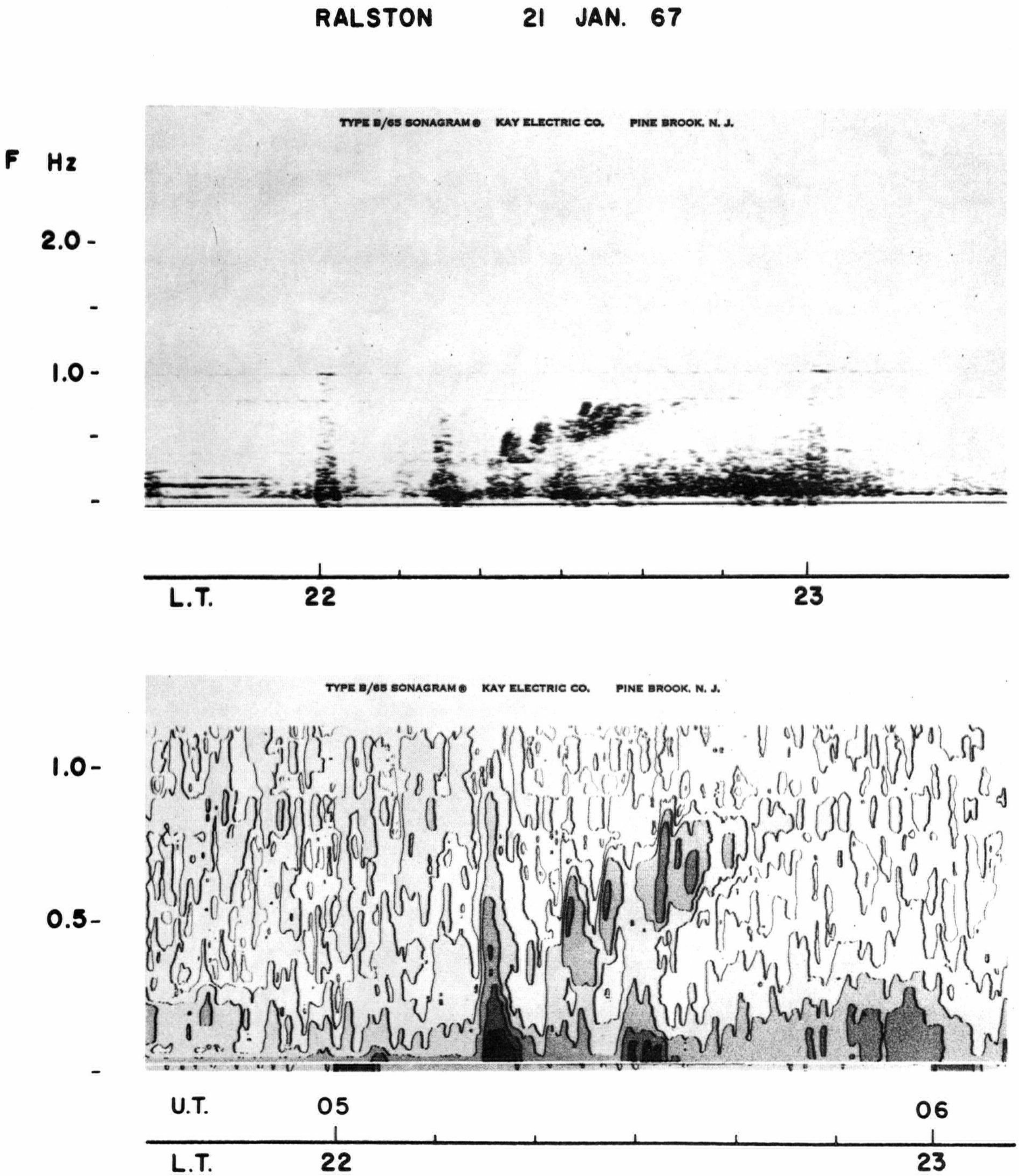

Fig. 8. IPDP with distinct structural elements

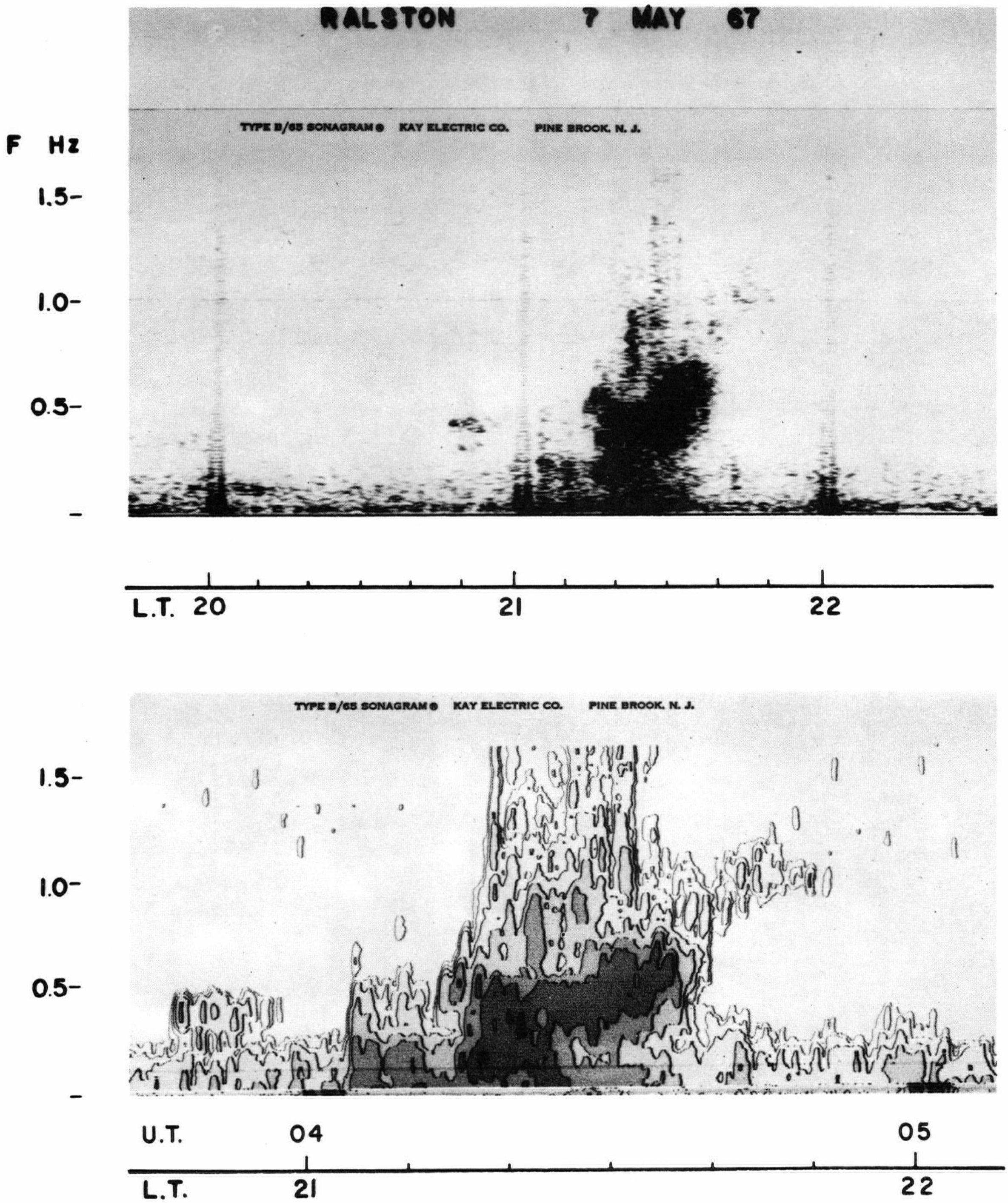

Fig. 9. IPDP with large noise band characteristic

the minimum or maximum frequencies observed so the above estimates are only approximate. Palo Alto IPDP's had approximately the same limits except for a few cases having a larger maximum frequency ($\sim$ 2.0 hertz). This suggests some geomagnetic control of IPDP frequency and confirms the observation of Knaflich and Kenney (1967) that IPDP's at Seattle (53.6°geomagnetic latitude) extend to higher frequencies than the same IPDP at College (64.6° geomagnetic latitude). Care must be taken in any comparison though, as different recording equipment has been used at all four stations.

The rate of increase of IPDP midfrequency varies from a very small value to about 5 hertz/hour, 0.3 hertz/hour being a typical value. The rate of increase is generally large for IPDP's near local midnight but large rates of increase also occur at other times. No relationship has been found between rate of frequency increase and local time, Kp index, or amplitude of event.

IV.3 Occurrence of IPDP's

The occurrence of IPDP's depends strongly on the local time of the observing station. Fig. 10 and 11 show the number of IPDP's observed in any one hour interval versus the local time. Most IPDP's occur in the 16 to 22 hour local time interval which is the dusk to midnight quadrant in the magnetosphere. This

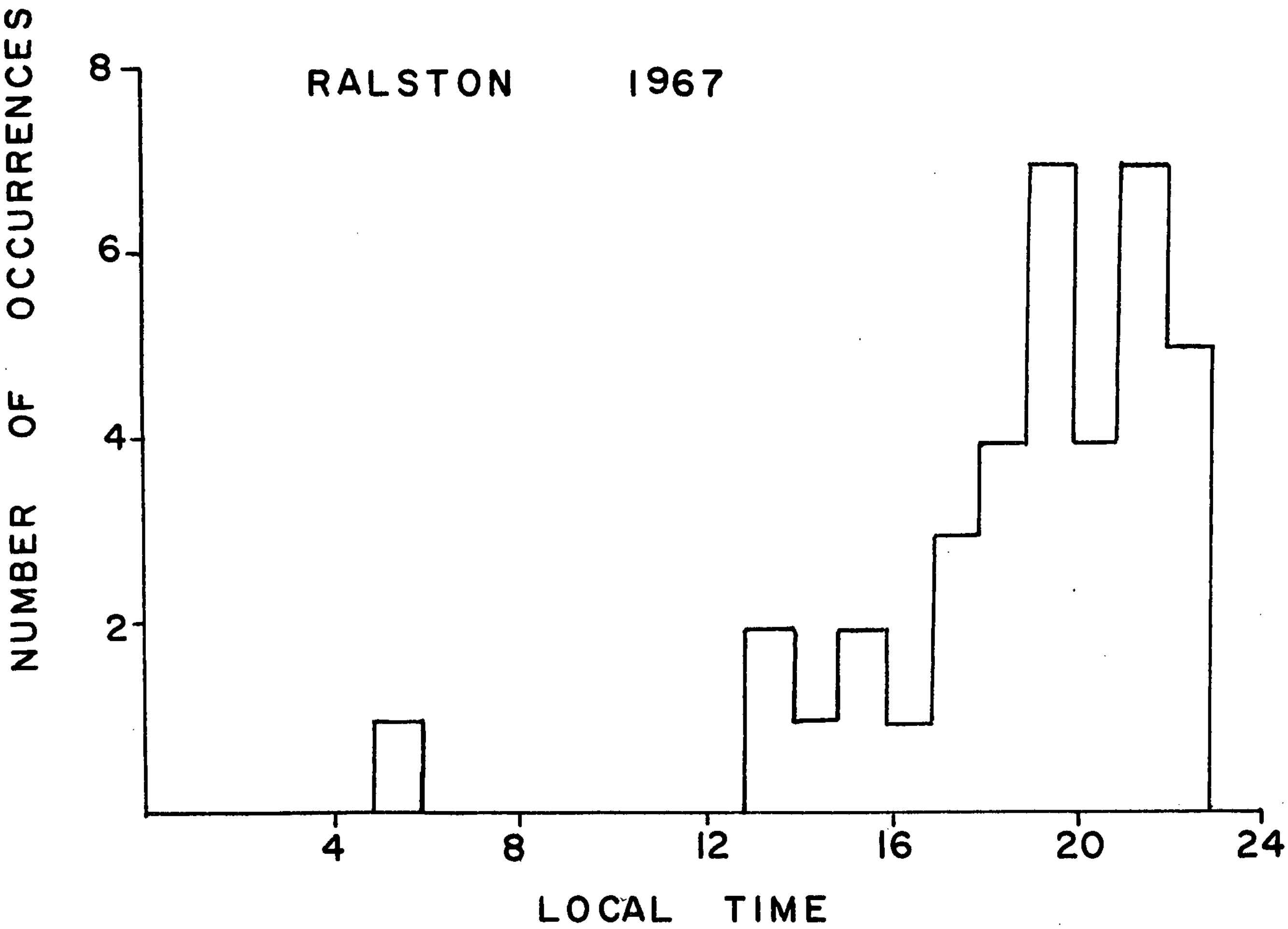

Fig. 10. Occurrence of IPDP's at Ralston versus local time

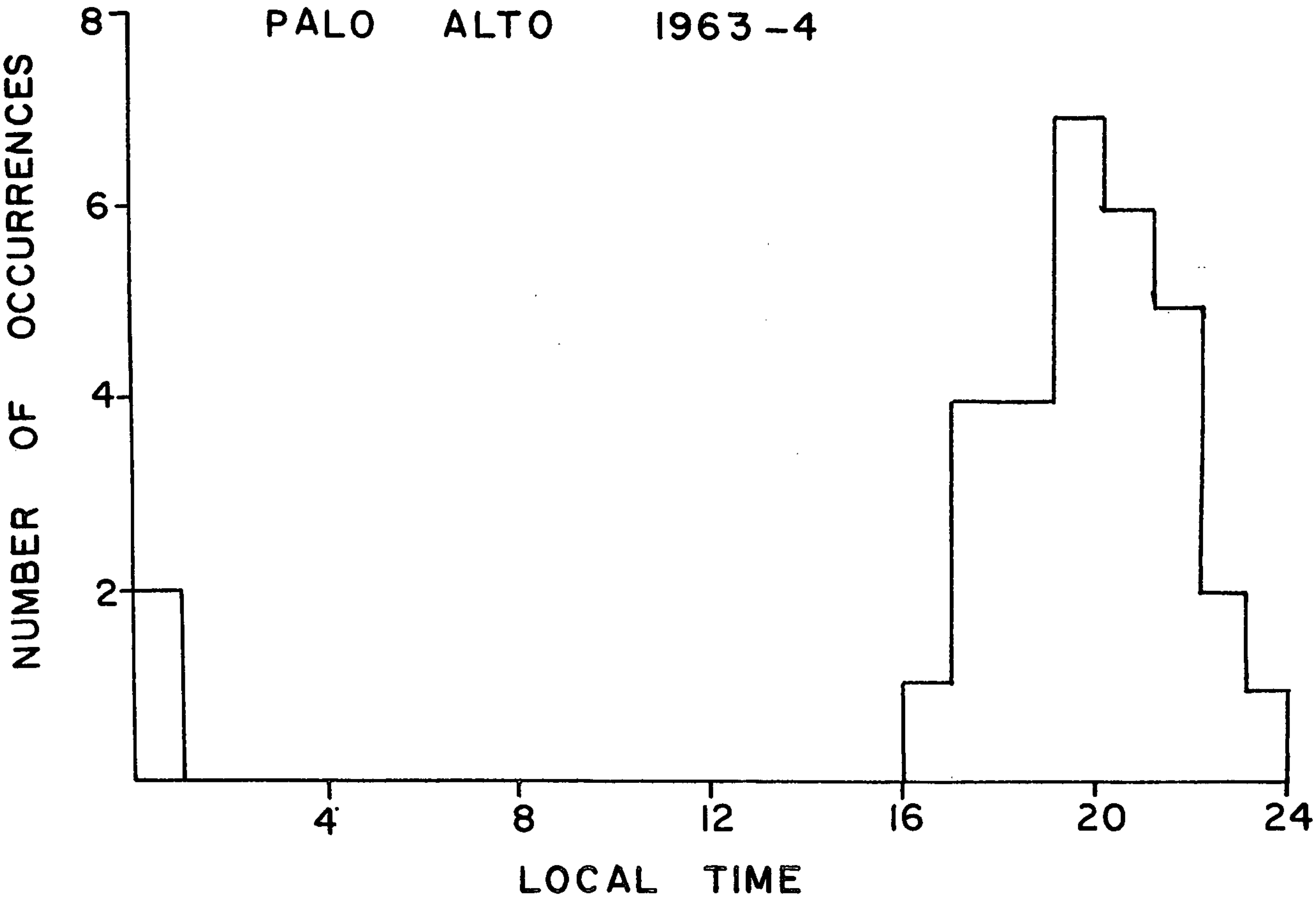

Fig. 11. Occurrence of IPDP's at Palo Alto versus local time

strong maximum also means that any one IPDP is visible only over a restricted longitudinal range. This range may be as large as 30° though, since the same IPDP has been observed at College and Seattle (Knaflich and Kenney 1967). An east-west line of micropulsation stations would be necessary to define the exact longitudinal extent of IPDP's.

Ralston and Palo Alto occurrence frequencies are very similar but Palo Alto IPDP's occur during more magnetically disturbed conditions as Fig. 12 shows. The solid lines show the number of IPDP occurrences versus Kp index (a measure of planetary magnetic activity), whereas the dashed lines are the number of occurrences normalized to the number of 3 hour Kp indices observed between 1800-2400 L.T. for the year(s) in question. The scale for the normalized occurrence rates is given on the right hand side of the figure.

Upon examination, Fig. 12 shows that the average Kp index for IPDP events at Palo Alto (5_{o}) is larger than for events at Ralston (4-). At both stations, however, the normalized occurrence of IPDP's increases for increasing Kp index. Also, the total number of IPDP's observed is larger at Ralston and still larger at College (Heacock 1967a). Thus, IPDP's must be a relatively high latitude phenomena or occur on high latitude field lines. They are correlated to magnetic activity as measured by the Kp index, and during times of large magnetic disturbances, the generation region likely

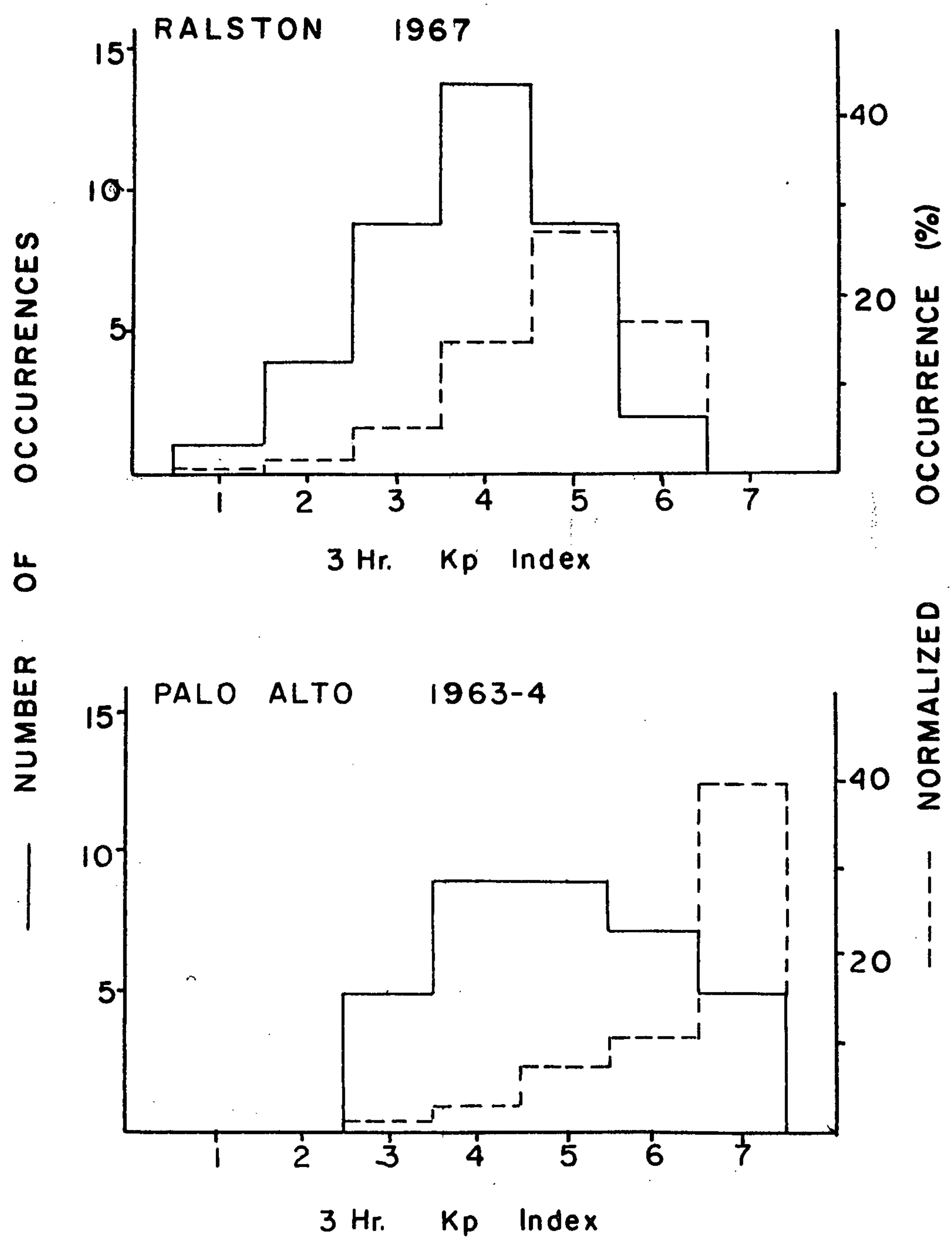

Fig. 12. Occurrence of IPDP's at Ralston and Palo Alto versus 3 hour Kp index

moves towards the equator (inward in the magnetosphere). Low latitude stations would observe IPDP's due to their propagation through the ionospheric duct (Tepley and Landshoff 1966, Manchester 1966, Greifinger and Greifinger 1968). No correlation has been found between magnitude of the IPDP and Kp index.

By incorporating the results of Section IV.5 in which IPDP's are found to be directly correlated with the occurrence of magnetospheric substorms, one can easily understand the increase in normalized occurrence rate versus Kp index. The Kp index is determined by averaging the K index (magnetic disturbance after various corrections) for 12 observatories which are located between 47.7 and 62.5 degrees geomagnetic latitude. By far the most important disturbance in this latitude range is magnetic bay activity which is a manifestation of the magnetospheric substorm process. Magnetospheric substorms thus govern both the Kp index and the generation of IPDP's.

IV.4 Occurrence with Hm Emissions

Occasionally IPDP's are observed with an hm emission following the increasing frequency noise band. Gendrin et al. (1967) mention this occurrence but do not give any quantitative figures. S. Lacourly (personal communication) reports that eleven, or 20% of the IPDP's observed at Kerguelen in 1965, were followed by an hm emission. However, for six months of available data in 1967, only 1 of 15 events ended in an hm emission.

No such cases were found in the 1967 Ralston data, but one case was found in the Palo Alto data. Knaflich and Kenney (1967) also have reported a couple of examples of this occurrence. Thus it has been firmly established that occasionally an hm emission directly follows an IPDP.

Fig. 13 shows the Palo Alto example indicating that the two types of pulsations are continuous in time. The IPDP starts at 07:40 U.T. and the hm emission starts at about 08:00 U.T., and is clearly visible at the end of the event. The gap preceding the frequency-time mark at 08:00 U.T. is not of natural origin.

Hydromagnetic emissions have been extensively studied, and are generally believed to originate from, or be amplified by, a cyclotron instability process between energetic protons and ion cyclotron waves (left-hand polarization) which are bouncing between a pair of magnetically conjugate areas under the guidance of the magnetic line of force connecting those areas (Jacobs and Watanabe 1964a, Obayashi 1965, Jacobs and Watanabe 1966). The continuity of the two events in Fig. 13 makes it likely that energetic protons are involved in the generation process of IPDP's, perhaps also via a cyclotron instability process.

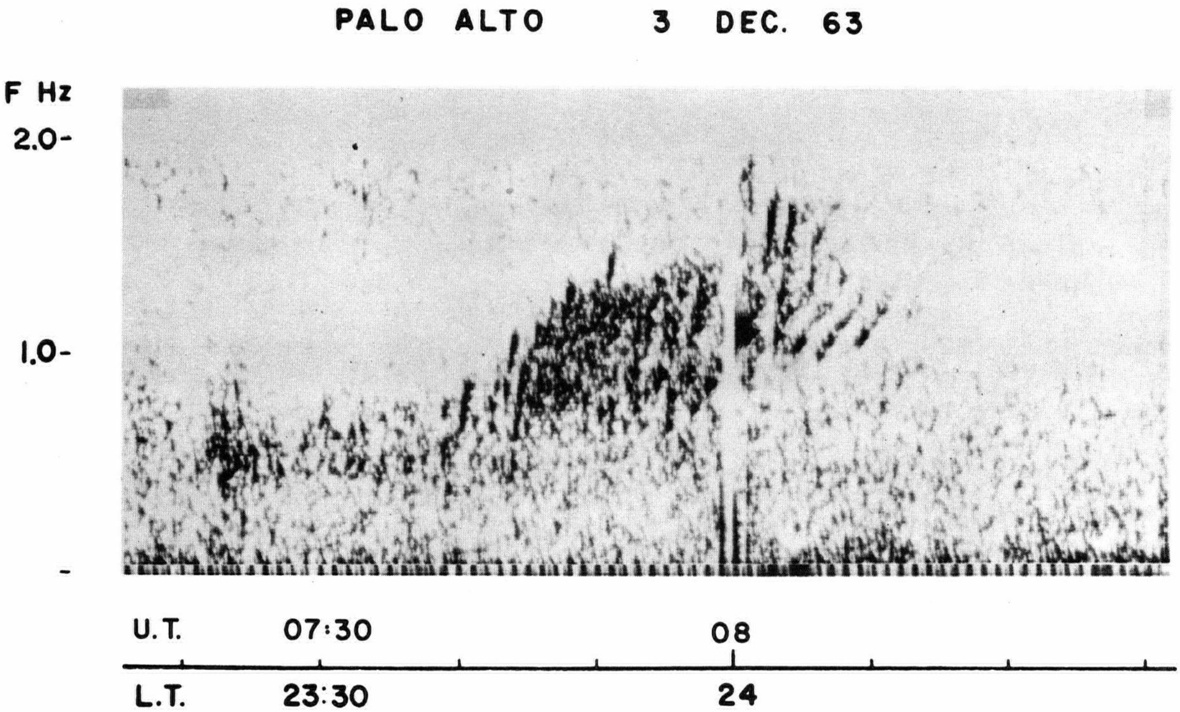

Fig. 13. An example of an IPDP which changes into an hm emission

Hydromagnetic emissions of the dispersive type, or hydromagnetic whistlers (Jacobs and Watanabe 1966), have been used to determine the equatorial radius to the guiding geomagnetic field line as well as the electron density at that point (Watanabe 1965, Dowden and Emery 1965). The December 3, 1963, example yielded a radial distance of 6.5 earth radii (Re) using Watanabe's (1965) method. Because of the short duration of the hm emission and the small amount of dispersion measured, the possible error will be quite large, say ±1 Re or more.

This estimate of generation region for IPDP's agrees closely with that of previous researchers. Gendrin et al. (1967) made an estimate of 3 to 6 Re by studying the occurrence of an IPDP at stations of varying latitude. They mention, however, that their estimate could be low due to the possibility of signal propagation in the ionospheric waveguide.

Knaflich and Kenney (1967) studied the structural elements of IPDP's and arrived at an estimate of 6 to 13 Re to the generation region. They had to assume that IPDP structural elements are half-hop micropulsation whistlers generated by a broad band impulse at the equatorial plane. Also, the plasma density distribution and magnetic field configuration was assumed to be undisturbed by the occurrence of a magnetospheric substorm. Both assumptions may not be valid.

In order to obtain an accurate estimate of distance to generation region, more examples of IPDP's followed by hm emissions are needed. But, by using the radial estimate made here and the occurrence of IPDP's versus local time, one can deduce the generation region of IPDP's. This region is illustrated in Fig. 14 which is an equatorial plane view of the magnetosphere.

IV.5 Relationship to Magnetospheric Substorms

Troitskaya (1961), Heacock (1966), Gendrin et al. (1967) and others have noted that IPDP's generally occur during times of magnetospheric activity. Since a great many phenomena are observed during the lifetime of a substorm, a more exact correlation must be looked for between some substorm process and the occurrence of IPDP's.

The analysis of magnetograms from auroral zone observatories is one of the most common ways of observing and studying magnetospheric substorms. Chapter III showed that magnetograms from a world-wide network of observatories can be used to identify the various phases of substorms. In this section it will be shown how the expansive phase has been picked for both simple and complex substorms and how the occurrence of IPDP's is related to this phase. Magnetograms from all the observatories listed in Table II.2 were used to identify the expansion phases of substorms studied. For ease of illustration only a few magnetograms are shown for each example.

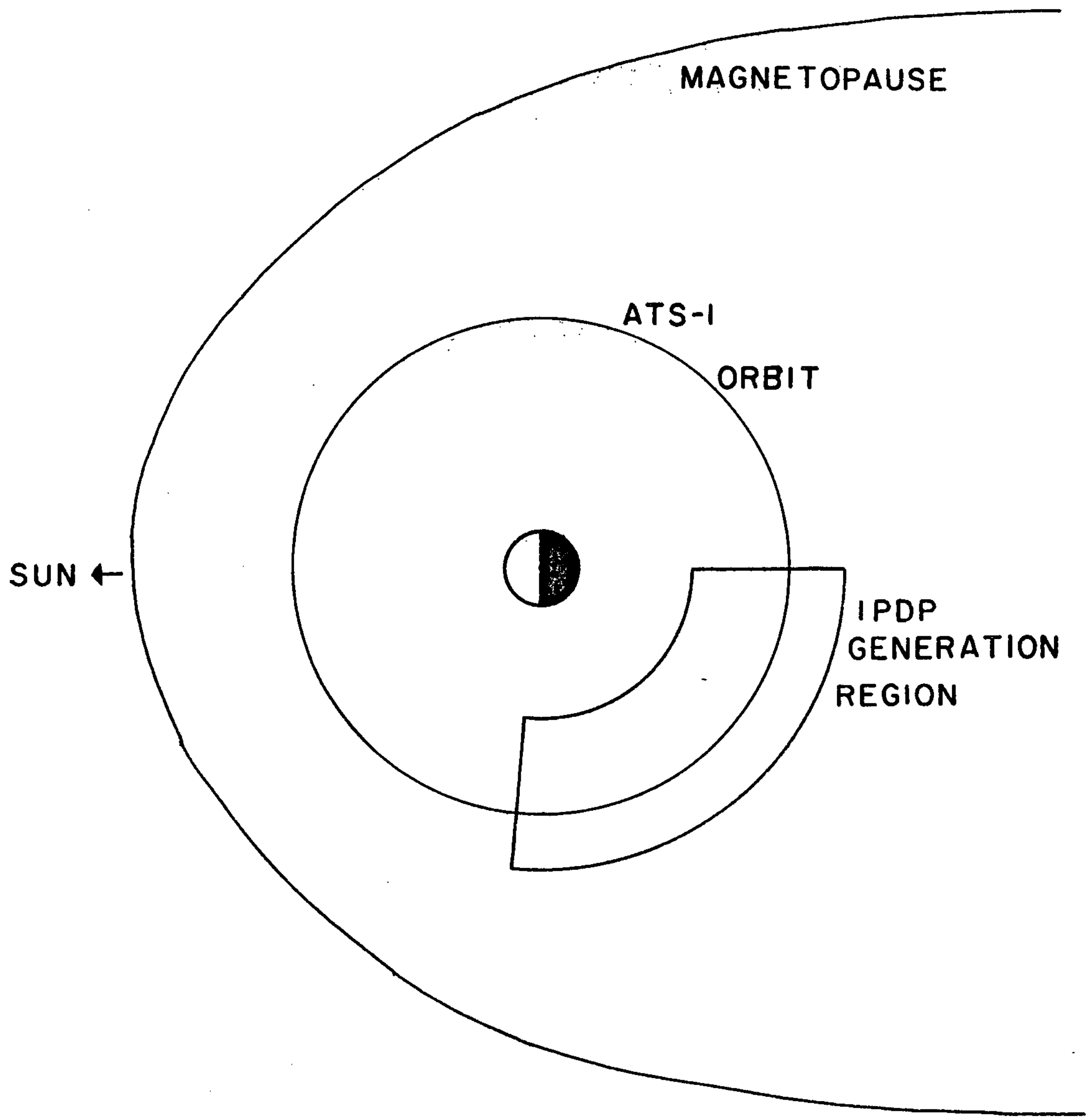

Fig. 14. IPDP generation region sketched in an equatorial plane view of magnetosphere

Fig. 15 is a set of magnetograms for January 21, 1967 with the corresponding IPDP shown in Fig. 8. Although this substorm produced a relatively simple magnetic bay in the dusk region, the two stations nearest midnight, Churchill (not shown) and Great Whale, do not show any clear evidence of the substorm. However, a sharp change in several magnetograms is seen at 05:25 U.T., thus indicating the start of the expansive phase at that time. The slow increase in College horizontal field from 05:00 to time of expansion is likely associated with the quiet or build-up phase of the polar magnetic substorm. This is an example of a relatively simple substorm but the absence of a magnetic disturbance at Churchill and Great Whale might mean that the equivalent current system, and thus the real current system, is unusual.

Fig. 15 also shows the H component of magnetic field at ATS-1. Note that the field recovery at ATS-1 started at 05:25 which is precisely the starting time of the Ralston IPDP and the expansive phase as defined by ground magnetograms.

The magnetograms of Fig. 16 illustrate a more complicated substorm period occurring on March 18, 1967. The substorm starting at 03:25 U.T. is evident at all stations shown as well as at Boulder, Fredericsburg, and Baker Lake and thus conforms to the idea of a large equivalent current system. At 04:20 U.T. another substorm is visible at Great Whale, Churchill, Boulder and Baker Lake but not at other stations. However, Fredericsburg,

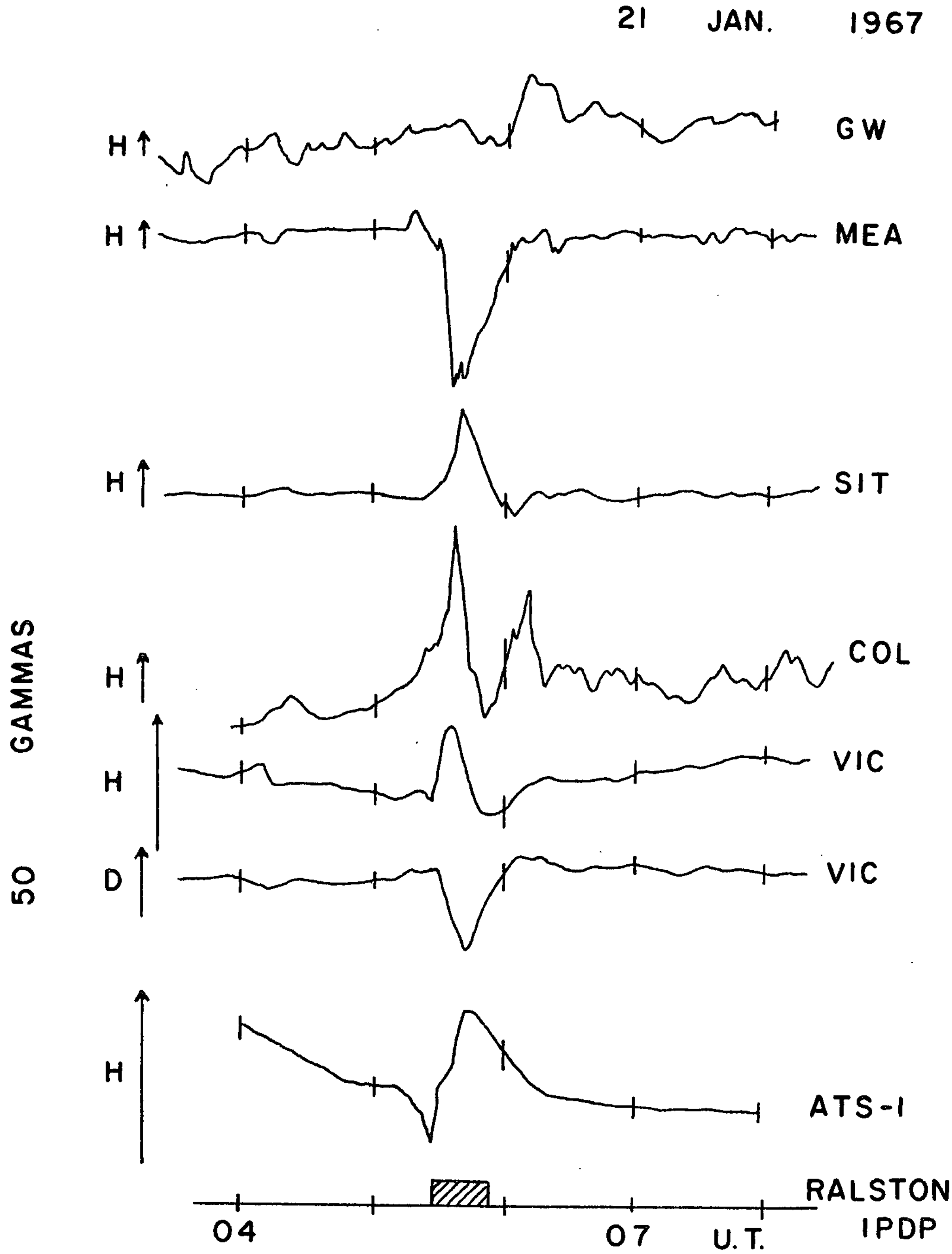

Fig. 15. Example of IPDP occurrence during a polar magnetic substorm

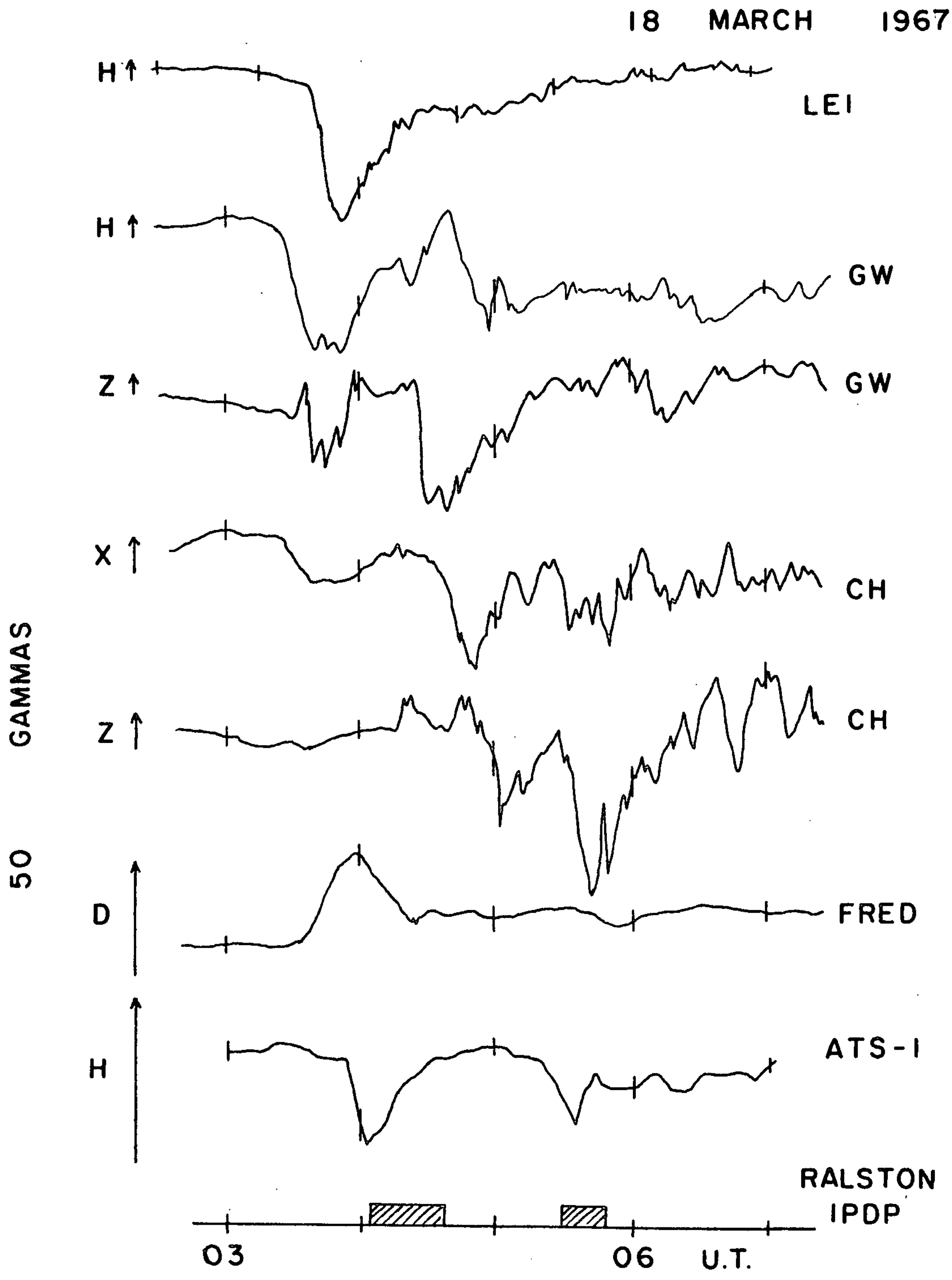

Fig. 16. Example of IPDP occurrence during a complicated substorm period

Victoria and several other observatories show a Pi 2 event starting at 04:15 which, according to Angenheister (1912), Terada (1917) and Rostoker (1966), is generated at the start of a substorm. The Churchill magnetogram has another major excursion at 05:25 U.T. but no other station records a significant magnetic field change at that time. However, a possible Pi 2 event is observed at about 05:30 U.T. on the Ralston micropulsation chart recording. The large difference between Great Whale and Churchill magnetograms and the lack of a disturbance at other observatories indicates the unusual character of the 05:25 substorm. For March 18, expansive phases would be at 03:25, 04:20 and 05:25 U.T. even though the latter two cases are anomalous.

The ATS-1 magnetogram for March 18 also does not follow the general picture given in Chapter III. The first two substorms are combined into one at ATS-1. No large change is observed until 03:50 at which time the field starts depressing. The recovery starts at 04:00 and lasts until 04:30 or later. This depression and recovery is likely due to the 03:25 substorm, the recovery at ATS-1 being delayed 35 minutes from the start of the substorm expansive phase. The second substorm at ATS-1 has its recovery phase at 05:30 and thus corresponds to the substorm observed only at Churchill. While the ground magnetic changes were observed only at Churchill (23 L.T.), the asymmetric ring current was observed in the dusk region (18 L.T. at ATS-1). What is most important to observe for this complex case is that IPDP's occurred simultaneously with the field recovery at ATS-1.

Fig. 17 is a set of magnetograms for April 17, 1967. The Great Whale magnetogram shows two substorms starting at 02:45 U.T. and 03:10 U.T., while the Churchill magnetogram indicates only one substorm at 03:05 U.T. The Ralston slow speed micropulsation recording reveals that Pi 2 pulsations occurred at 02:48 and 03:09 U.T., indicating two closely spaced substorms. The positive D bay at Boulder coincides with the first substorm. An IPDP was observed at Ralston precisely during the time of mid-latitude D bay and this correlation has been noted for the majority of IPDP's. The difference between the magnetic effects of the two substorms at Boulder, which is well south of the auroral zone, means that the current systems of the substorms were also quite different.

Again the Ralston IPDP occurred during the time of field recovery at ATS-1. However, an IPDP was not observed during the second field recovery. The significance of this observation will be discussed in Section V.1. The sonagrams for the IPDP's discussed in the previous two examples are shown in Fig. 18 and 19.

The preceding examples indicate a correspondence between IPDP occurrence and the expansive phase of a substorm. Fig. 20 plots the starting time of all Ralston IPDP's relative to the time of substorm expansion. It clearly shows that IPDP's start at the time of substorm expansion or shortly thereafter. The ATS-1 field recovery is associated with the substorm expansion (Cummings et al. 1968), so Fig. 20 also implies that IPDP's

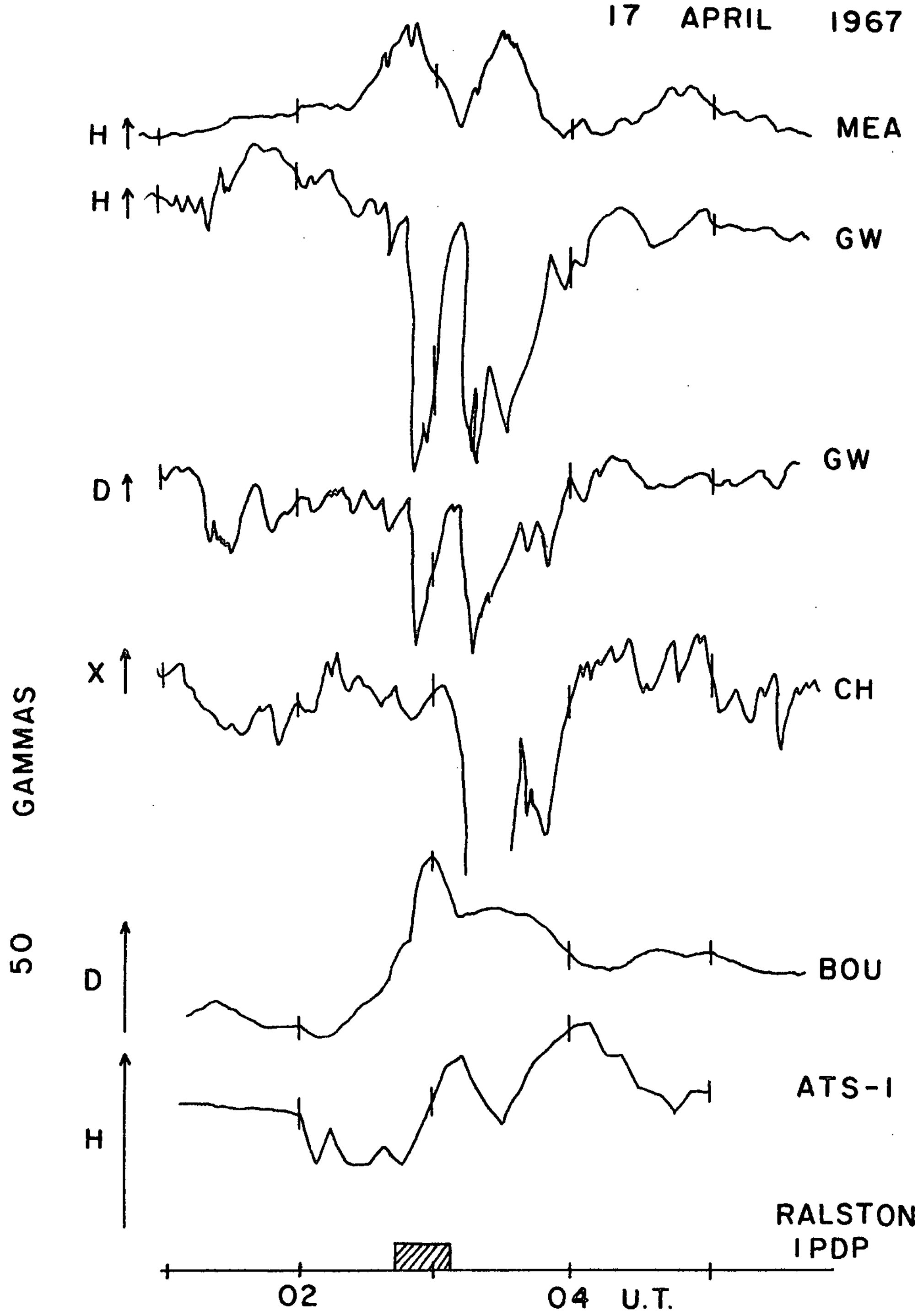

Fig. 17. IPDP occurrence during two closely spaced polar magnetic substorms

RALSTON 18 MARCH 67

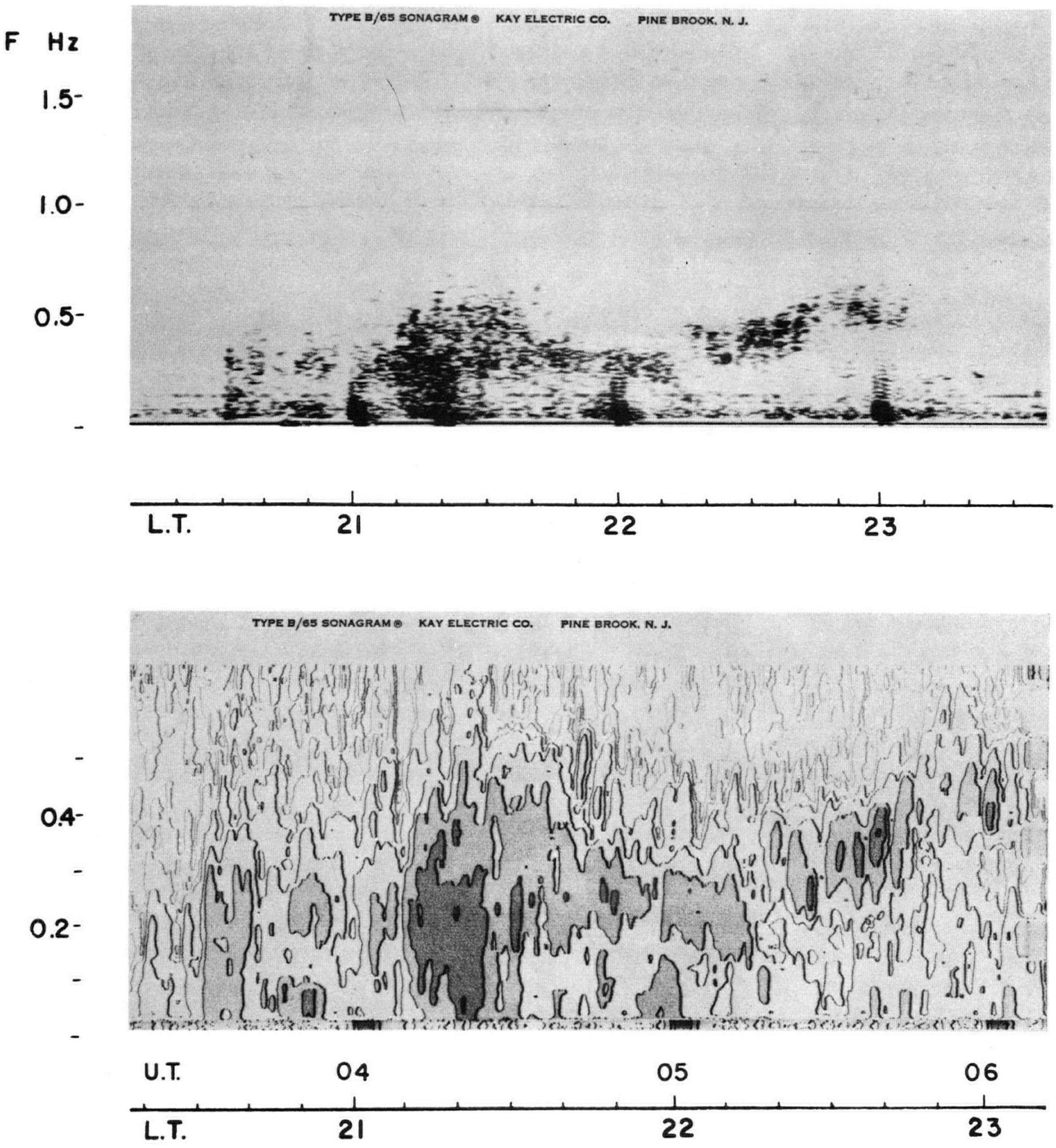

Fig. 18. IPDP event occurring during substorm shown in Fig. 16

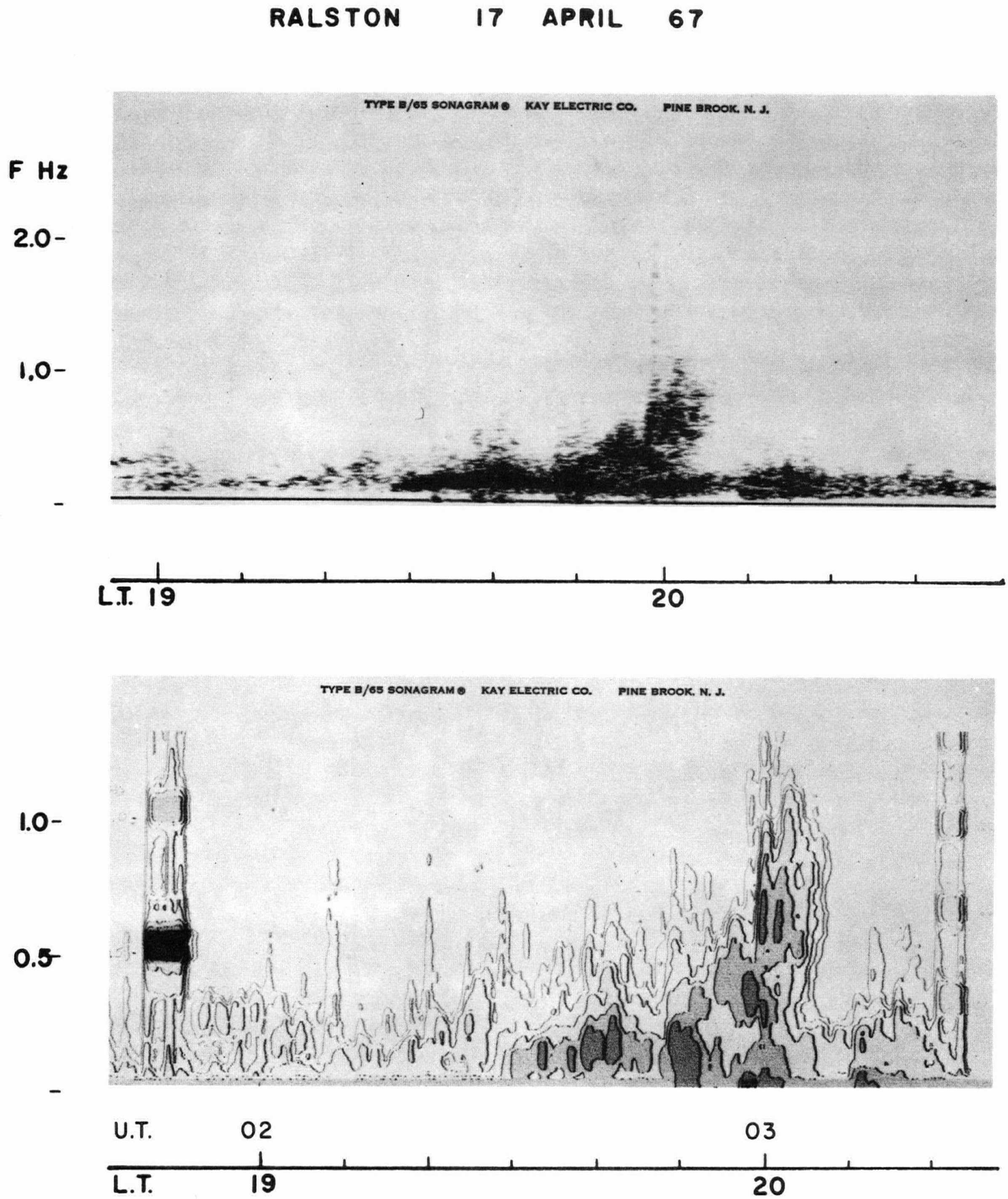

Fig. 19. IPDP event occurring during substorm shown in Fig. 17

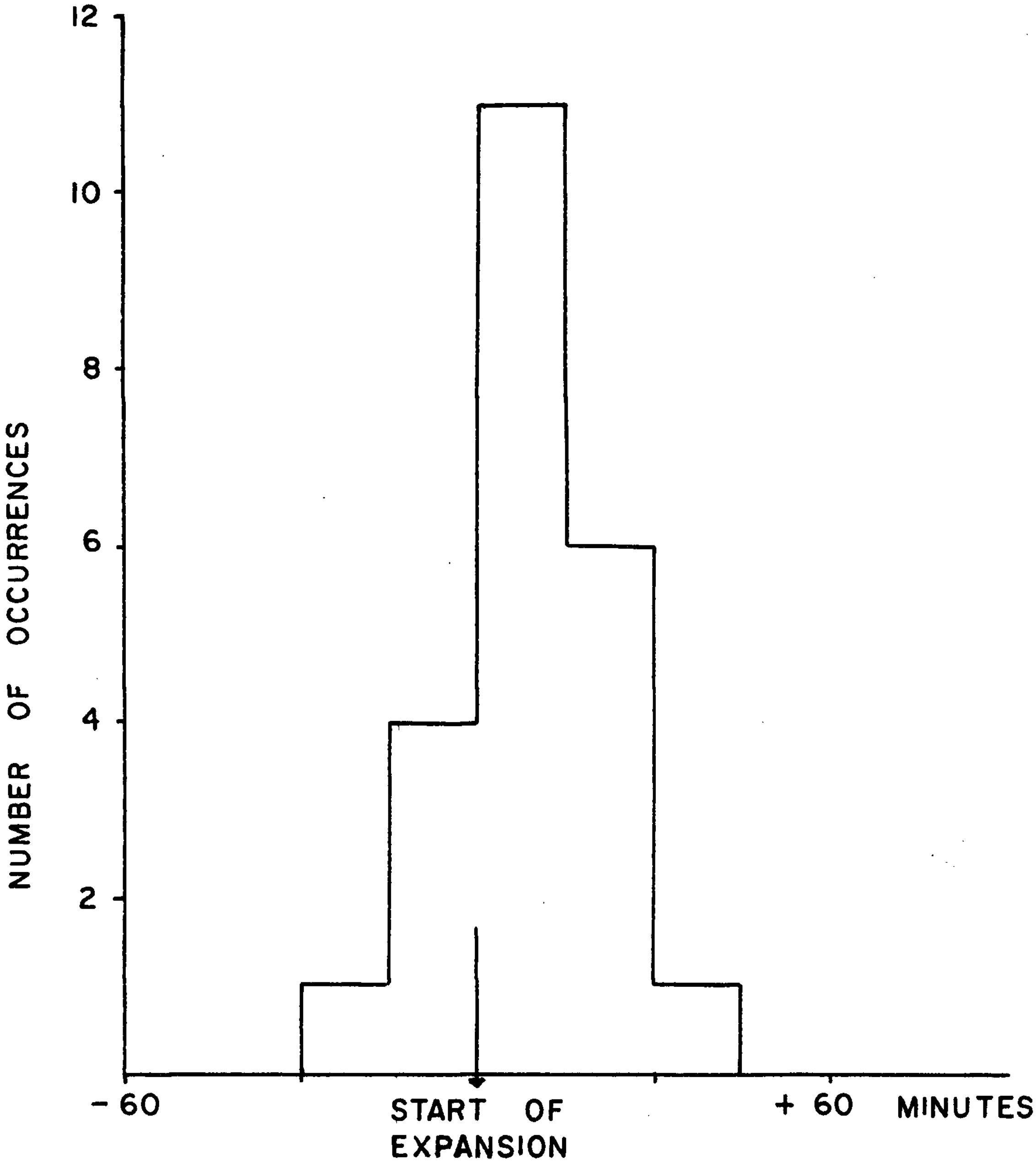

Fig. 20. Occurrence of Ralston IPDP's relative to time of substorm expansion

occur during the time of magnetic field increase in the dusk-midnight quadrant. Many other phenomena also occur during the substorm expansive phase but it will be shown in Section IV.6 that the magnetic field increase as observed by ATS-1 produces the frequency increase of IPDP's.

IV.6 Magnetic Field Control of Frequency Change

Section IV.4 pointed out that IPDP's are likely associated with a cyclotron instability between an ion cyclotron wave and energetic protons. Section IV.5 noted a correspondence between IPDP's and an increasing magnetic field at ATS-1. It is now proposed that the noise band of IPDP's is produced by a cyclotron instability process between energetic protons and an ion cyclotron left-handed wave. The increase in noise band midfrequency results from an increase in the background magnetic field in the IPDP generation region. In order to test this proposal the cyclotron instability process must be examined.

The dispersion equation for a left-handed ion cyclotron wave propagating parallel to the background magnetic field is: (Astrom 1950)

$$\omega^2 - c^2k^2 - \sum_{\text{comp}} \frac{\Omega_p^2\ \omega}{\omega - \Omega} = 0 \qquad (1)$$

where $$\Omega_p^2 = \frac{4\pi Ne^2}{m}$$

$$\Omega = \frac{qB_o}{mc}$$

and N , m , q are the number density, mass, and charge (with sign) of the plasma components, and B_o is the background magnetic field. The summation is over the components of the plasma which in the IPDP generation region can be considered to be electrons and protons. The usual assumption of a neutral plasma is also made, i.e., $N_e = N_i$.

A resonance can take place between an ion cyclotron L.H. wave and both protons and electrons. However, energetic protons are chosen as they have been proven to be the interacting particle in the case of hm emissions (Cornwall 1965, Gendrin 1965, Jacobs and Watanabe 1965, 1966). Protons will resonate with the hydromagnetic wave when their rotation about the field lines is at the same frequency as the wave frequency doppler shifted to the velocity of the protons parallel to the magnetic field lines. This is expressed mathematically as

$$\omega - ku = \Omega_i \qquad (2)$$

where u is the protons' parallel velocity and Ω_i is the ion cyclotron frequency.

Using the resonance condition (2) and the dispersion equation (1), a relationship between the background plasma density N_i, magnetic field B_o, the wave frequency ω, and the parallel energy of energetic protons can easily be derived (Appendix II)

$$N_i W_{\parallel} = \frac{e^2}{8\pi \; m_i^2 c^2} \left(1 - \frac{\omega}{\Omega_i}\right)^3 \frac{B_o^4}{\omega^2} \qquad (3)$$

Equation (3) can be used to find the instability frequency if all the other parameters are known. A much more complex analysis must be performed to determine the conditions for wave growth. This analysis has been performed by many authors (Cornwall 1965, Liemohn 1967, Jacks 1966) and is not necessary for this study.

The variation of the instability frequency ω can be seen more easily if we assume that $\omega << \Omega_i$. Then:

$$\omega \propto \frac{B_o^2}{\sqrt{N_i W_{\parallel}}} \qquad (4)$$

The instability frequency will increase if B_o increases or if N_i or $W_{\parallel}$ decreases.

Equation (3) can now be used to test the hypothesis that an increase in B_o produces the frequency increase of an IPDP. Magnetic field data were available from the ATS-1 satellite for nine IPDP's (Table IV.1) observed at Ralston. For each

Table IV.1

IPDP's Used for Frequency Versus Magnetic Field Study

Date	Start Time L.T.	Δf hertz	ΔB γ	ΔT Min.
Jan. 21	22:25	.22	38	15
March 18	22:30	.06	10	10
March 27	21:15	.13	13	20
April 17	19:55	.28	15	15
May 7	21:15	.24	6	15
May 16	22:20	.11	7	5
May 17	21:55	.18	8	20
Aug. 14	19:50	.12	3	5
Sept. 13	21:35	.03	7	10

event the midfrequency was measured from the contoured sonagrams at intervals of five minutes. The frequency thus determined was plotted against the observed total magnetic field at ATS-1 with time as the parameter (Fig. 21). (See Appendix III.)

The solid curves in Fig. 21 represent lines of constant $N_i W_{\parallel}$. The plasma density in the IPDP generation region is of the order of 1 particle/cm^3 (Carpenter 1966) so the curves represent approximately parallel energy (kev) of resonating protons. If the IPDP's observed at Ralston were generated in the vicinity of the ATS-1 satellite and if all the frequency change observed was due to an increase in the background magnetic field, the individual events should follow the curves of constant $NW_{\parallel}$. Many of the events do approximately follow the theoretical curves. For these events, all the observed frequency increase is explained by the magnetic field increase as observed by ATS-1.

For some IPDP's the magnetic field seen by the resonating protons may not be the field measured by ATS-1. A correction must be made for the satellite's motion, and thus measurement of $\frac{D\vec{B}}{Dt}$ due to $(\vec{v}\cdot\nabla)\vec{B}$. Also, if the IPDP is not generated near the satellite a positional correction will be needed. Only the first correction can be made on a quantitative basis.

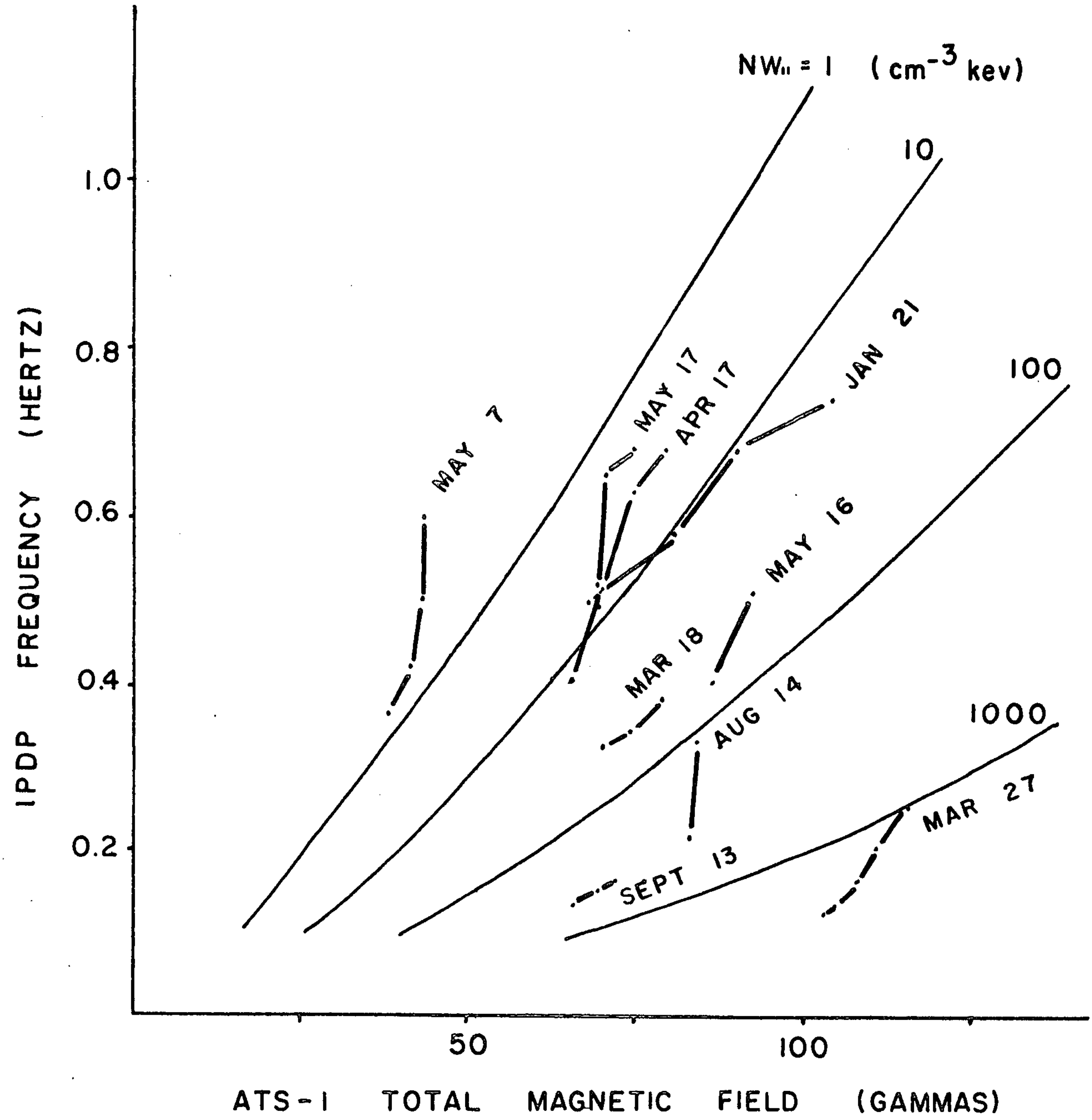

Fig. 21. Ralston IPDP frequency increase relative to ATS-1 magnetic field change with time as the parameter

The magnetic field measured by ATS-1 exhibits a diurnal variation just as a ground magnetic observatory does. However, the variation is not constant but depends on the parameters of the magnetosphere such as subsolar distance to magnetopause, distance to tail current sheet, and tail magnetic field strength. The diurnal variation for March 18, 1967 is illustrated in Fig. 22. The H component at ATS-1 decreases from a maximum of 155 γ at noon to a minimum of less than 50 γ at midnight. The dashed line is a Mead's model (Mead 1964, Williams and Mead 1965) approximation of the diurnal variation. The parameters used are subsolar distance to magnetopause 8.0 Re, distance to tail current sheet 9.6 Re, termination of current sheet 117 Re, and tail field 60 γ. The diurnal variation on a magnetic quiet day (March 11) is also shown in Fig. 22.

Two important facts are evident. The large decrease in the dusk region is due to the satellite's motion into regions of lower magnetic field. This decrease must be taken into consideration when the field change at one position is desired. Secondly, the amount of correction necessary varies extremely as evidenced by March 11 and 18. The correction for March 18 at 04:00 U.T. is +14 γ/hour which is the negative slope of the tangent to Mead's model curve at that time, while the correction for March 11 is only +1.5 γ/hour.

Unfortunately not all days exhibit steady magnetospheric conditions as does March 18. Often a major change such

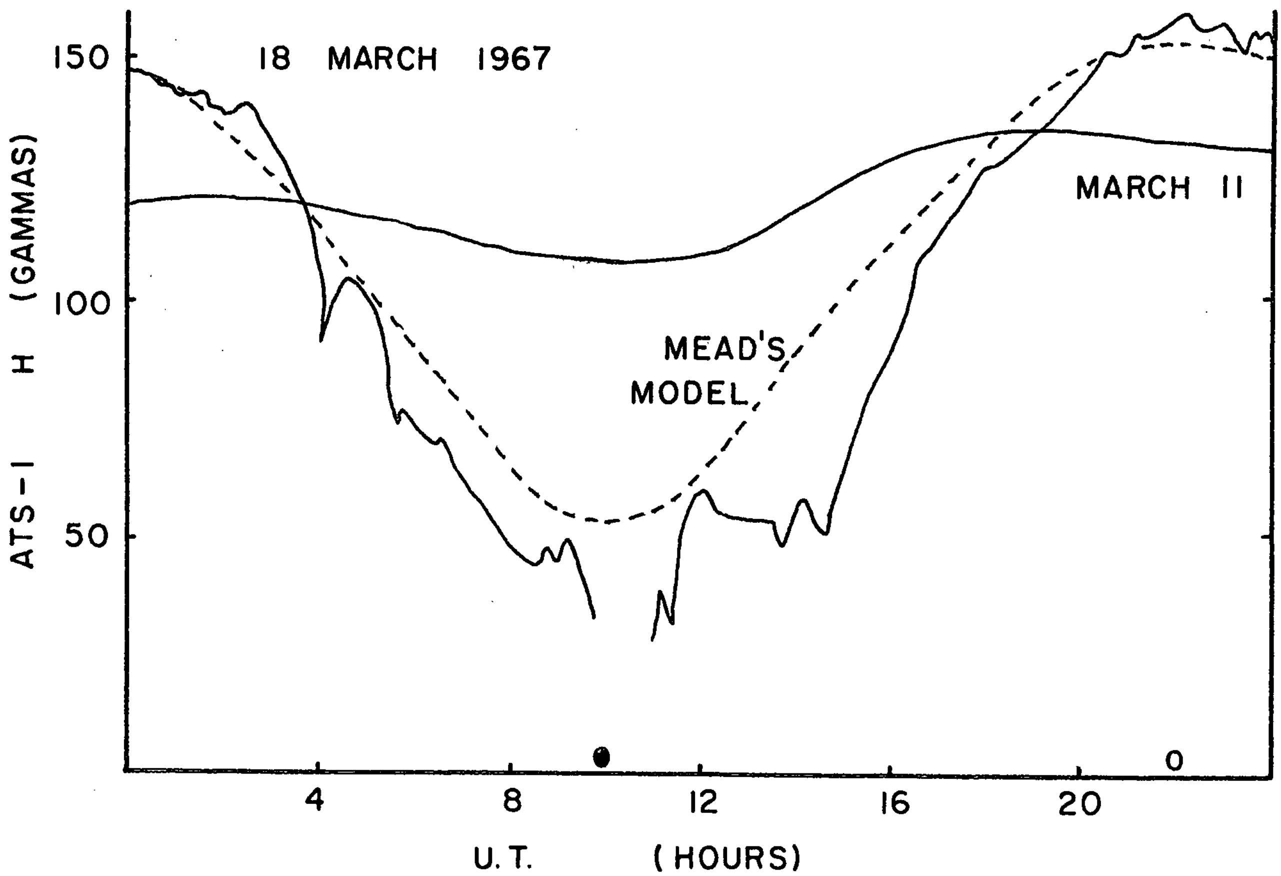

Fig. 22. Diurnal variation of H component of magnetic field at ATS-1 for a quiet and a disturbed day

as the magnetic storm on May 7, 1967, makes it impossible to determine a diurnal correction. However, May 7 was the only example of the events used in Fig. 21 for which a correction could not be determined.

The correction for relative position of satellite and IPDP generation region is difficult because the spatial variation of magnetic field changes during a magnetospheric substorm is unknown. But the three hour L.T. difference between Ralston and ATS-1 could be important since there is sometimes a delay in field recovery at ATS-1 from the time of substorm expansion. When the satellite is at midnight the field recovery starts simultaneously with the substorm expansive phase (Cummings et al. 1968). Thus if an IPDP is generated in a longitudinal zone substantially closer to midnight than the position of ATS-1, a time delay might also be seen between the start of IPDP at Ralston and field recovery at ATS-1. The May 17 example of Fig. 21 may be such a case since the field recovery at ATS-1 occurs 25 minutes after start of substorm expansion and 15 minutes after start of Ralston IPDP. A correction of this type must be considered speculative at this time.

Fig. 23 is a repeat of Fig. 21 with corrections made for movement of satellite assuming IPDP's are generated at a fixed point in the magnetosphere. Also shown is the possible change in the May 17 example with a 15 minute time shift. The correspondence between the theoretical curves and experimental

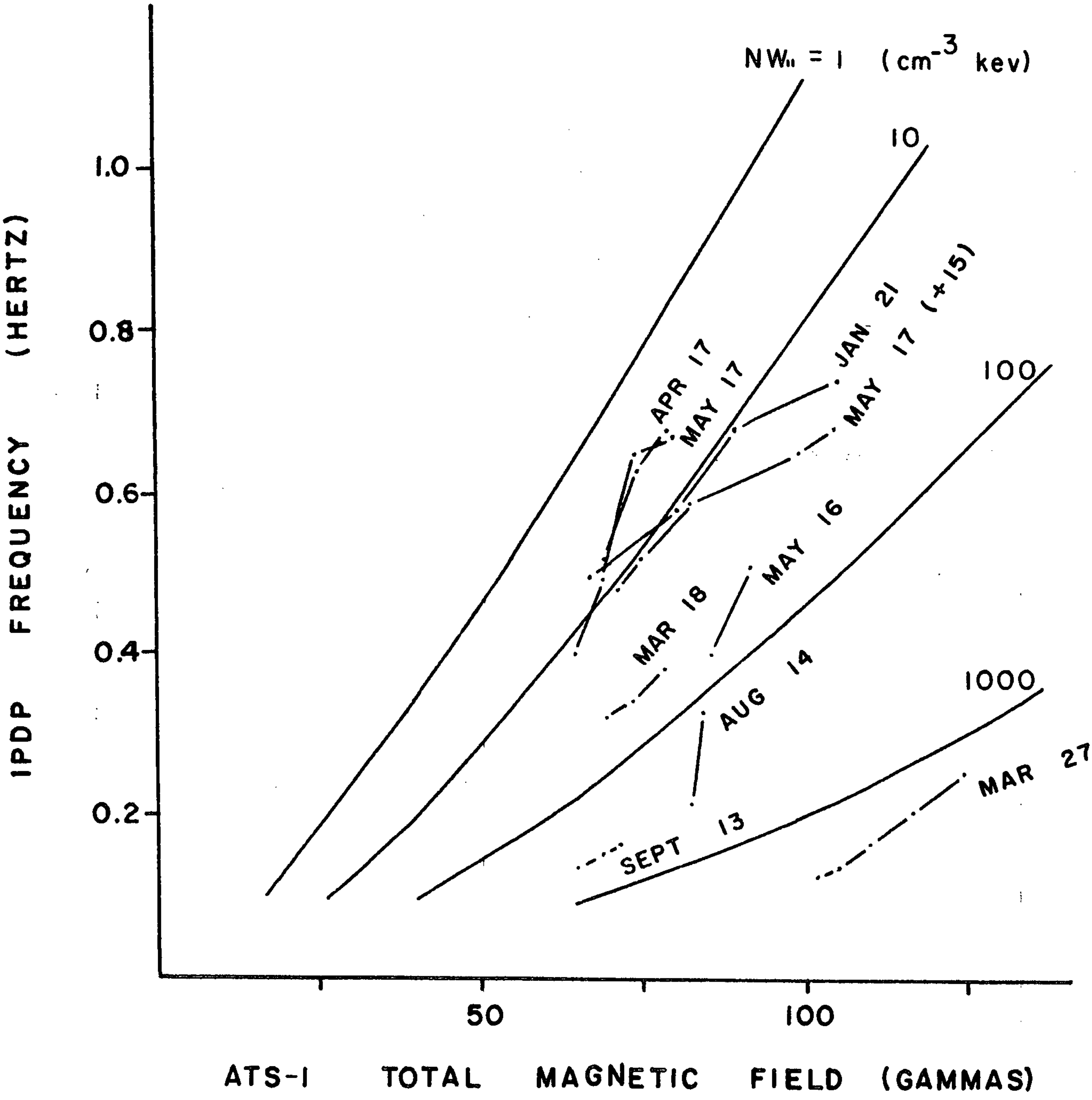

Fig. 23. IPDP frequency increase relative to ATS-1 magnetic field change with a correction for satellite's motion

data is greatly improved.

The May 7 example has been omitted since no correction was possible. During that time magnetospheric conditions were very disturbed as evidenced by the low magnetic field at ATS-1 (30 γ at 18:00 L.T.) and the satellite was likely not in IPDP generation region.

It can now be stated that the principal cause for the frequency rise observed in IPDP's is an increase in the background magnetic field thus changing the conditions for the cyclotron instability process. Other conditions influencing the production of an IPDP will be considered in the following chapter.

CHAPTER V

Discussion of IPDP Theories

V.1 Increasing Magnetic Field Theory

Chapter IV showed that the generation of IPDP's could be explained by a cyclotron instability between protons and ion cyclotron left-hand polarized waves under the control of an increasing magnetic field. Conditions on the resonating particles, the magnetic field, and other magnetospheric properties necessary for the initiation of an IPDP will be discussed in this section. The relationship between IPDP's and other micropulsations thought to be generated or amplified by a cyclotron instability process will then be discussed.

The magnetic field increase in the generation region of IPDP's produces their major distinguishing feature, i.e. the rise in average frequency of noise band. The general features of substorm associated, magnetic field changes, as measured by ATS-1, will be summarized here for a comparison with IPDP data.

Major magnetic field changes associated with substorms are seen only in the dusk-midnight quadrant of the magnetosphere. The field slowly becomes depressed some time before a substorm expansion occurs and at the time of expansion the field rapidly recovers. The recovery is gradual in the dusk region, quickest just before midnight, but completely absent after midnight local time (Cummings and Coleman 1968).

Cummings et al (1968) propose a partial ring current in the dusk-midnight quadrant as sketched in Fig. 24 to explain these effects. The magnetospheric current is composed of energetic protons drifting westward due to the gradient and curvature of the magnetic field. It is assumed that the electrons are either precipitated more quickly than the protons or that they are considerably less energetic. The current is carried to the ionosphere, and from the ionosphere along the earth's field lines. This partial ring current would exist mainly outside the orbit of ATS-1 and as it increases in magnitude, the magnetic field would become depressed at ATS-1. At the time of the substorm expansive phase a major portion of the ring current near midnight would be suddenly removed. The ring current at dusk would then decrease slowly due to the absence of a source of protons.

Note that these magnetic effects are confined to the IPDP generation region as defined in Section IV.4. Also note the sharp cut-off near midnight of the occurrence of IPDP's at both Ralston and Palo Alto (Fig. 10 and 11) corresponding to the cut-off of magnetic field effects as observed at ATS-1.

Energetic protons are also necessary for the generation of an IPDP as they supply the energy for growth of the ion cyclotron waves. An examination of Fig. 23 reveals that 10 to 1000 kev protons are most likely responsible for IPDP generation (since the background plasma density, $N \sim 1/cm^3$ in IPDP generation region). Studies of cyclotron-instability amplification

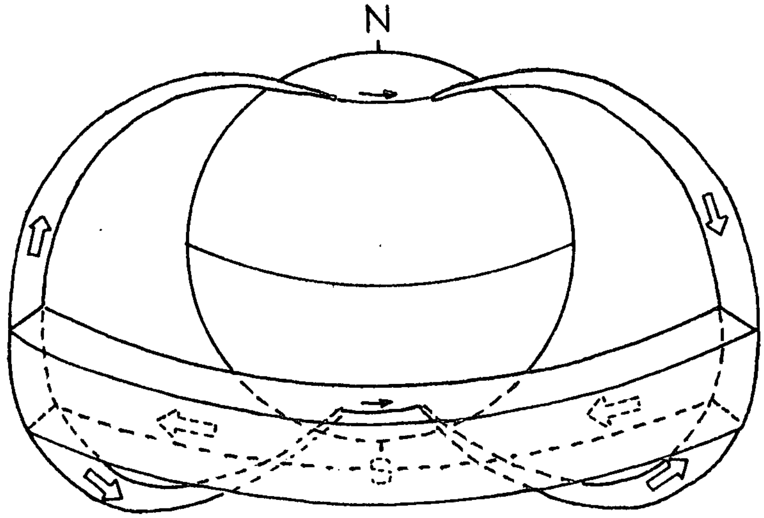

Fig. 24. Partial ring current existing during polar magnetic substorms as viewed from the dusk-midnight quadrant (after Cummings et al. 1968)

of hm emissions (Cornwall 1965, Liemohn 1967, Jacks 1966) reveal that 200 to 500 kev protons at L=4, or lower energy protons at larger L values, provide an efficient amplification of ion cyclotron waves. An anisotropic proton velocity distribution is needed for wave amplification but the existence of hm emissions of long duration is evidence for the existence of suitable protons in the magnetosphere. Since hm emission occurrence is enhanced after a magnetic storm (Tepley 1966), the protons may have been injected during times of strong substorm activity.

Substorm associated anisotropic proton velocity distributions have been observed by Konradi (1967, 1968) and Brown et al (1968). Measurements by Konradi (1967) indicate that the protons were injected into the night side of the magnetosphere from the tail region 15 to 20 minutes before the substorm expansive phase. These protons would drift westward and would be in IPDP generation region at time of substorm expansion. It is not known if the proton events observed by Konradi are the main source of IPDP energy but there certainly is no lack of protons with the proper energies at times of substorm activity.

Generally disturbed magnetospheric conditions may also influence the generation of IPDP's. Hydromagnetic emissions, 4-sec. period micropulsations, and IPDP's are all believed to be generated or amplified by a cyclotron instability process. Hydromagnetic emissions show a regular repetition of rising elements whereas 4-sec. period micropulsations and IPDP's consist of a noise band with irregularly spaced structures. The relatively quiet conditions existing during an hm emission may allow the amplification of an initial ion cyclotron "seed" wave to dominate the production of new waves. Under conditions of more magnetic noise, background plasma perturbations, and diversity of energetic particles, ion cyclotron waves may be continuously generated resulting in a noise band. Only occasionally would a large structural element be generated.

The simultaneous existence of resonating protons, increasing magnetic field, and magnetic noise or plasma turbulence would result in an IPDP. Different combinations of the three variables would result in other types of micropulsations such as hm emissions or 4-sec. micropulsations.

Magnetospheric substorms produce all three conditions in the dusk-midnight quadrant and thus IPDP's would be generated there. Constant frequency emissions often seen before or after IPDP's would be produced by a cyclotron instability process using the same proton source but with a static magnetic field. A good example of this magnetic field control of emission frequency is seen in the March 18 event (Fig. 16 and 18). A constant frequency emission resembling 4-sec. micropulsations separates the IPDP's occurring at 21:00 and 22:30 L.T. The magnetic field at ATS-1 was also approximately constant during this period.

Heacock (1967a) has published some excellent examples of 4-sec. micropulsations terminating in an IPDP. In those cases the resonating protons are introduced substantially before the substorm expansive phase. At the time of expansion the 4-sec. micropulsation changes into an IPDP.

Not all magnetic field increases observed at ATS-1 produced an IPDP at Ralston. For example, of the two field recoveries on April 17 (Fig. 17) only the first resulted in an IPDP. The lack of any Pc 1 frequency micropulsations during the second field increase would be due to the absence of suitable protons for cyclotron instability wave generation.

A most interesting combination of variables occurs when hm emissions are observed during a magnetic storm sudden commencement (ssc). The quiet magnetospheric conditions prevailing are suddenly changed to disturbed conditions by a sharp increase in the magnetic field. Heacock and Hessler (1965) show the sonagrams for hm emissions occurring during this period (Fig. 2 of their paper). The emission frequency takes a sudden jump at the time of ssc and then the structural elements disappear leaving a noise band. The jump in frequency and loss of structure of the emission has been caused by the sharp increase in background magnetic field and resulting disturbance of the plasma.

The structural elements observed in IPDP's offer special problems. They are usually observed simultaneously at conjugate stations (Gendrin et al 1967) but some elements occur with a slight time difference and others appear only at one station. Therefore, these elements cannot be given the same interpretation as those from hm emissions which appear alternately at conjugate stations.

The disturbed magnetospheric conditions existing in IPDP generation region can be used for a qualitative explanation of IPDP structure. The noise generation process may be enhanced suddenly either by an external impulse or by a change in resonance conditions at or near the equatorial plane. This amplitude enhancement or structural element, would propagate in both directions along the geomagnetic field line. Due to the distortion of field lines and plasma densities by the asymmetric ring current, the elements would arrive simultaneously or with a slight delay at conjugate stations. The energy reflected by the ionosphere is probably insignificant compared to the wave energy continually being generated in the equatorial region. If the wave (structural element) was generated significantly off the equatorial plane, the wave propagating back through the IPDP generation region may be damped by different resonant conditions existing there and only one hemisphere would see the element.

Certainly more experimental and theoretical work needs to be done on IPDP structures but until the magnitude and extent of magnetospheric disturbances are established, no quantitative analysis can be performed.

V.2 Other IPDP Theories

Previous to this work, two major theories for IPDP generation had been proposed. Both are based on a cyclotron instability between protons and ion cyclotron L mode waves, but different mechanisms are used to explain the noise band frequency increase.

Heacock (1967a) and Gendrin et al. (1967) explain the frequency rise by assuming that the resonating protons are diffusing inward across the geomagnetic field lines, thus moving into regions of larger magnetic field and background plasma density. The resulting change in IPDP frequency would be given by equation (4) of Chapter IV

$$\omega \propto \frac{B_o^{\,2}}{\sqrt{N_i W_{\parallel}}}$$

In the magnetosphere under steady state conditions, $N_i \propto B_o$, and if one assumes that the particles do not gain energy by the diffusion process, the emission frequency will be:

$$\omega \propto B_o^{\,3/2} \qquad (5)$$

in which B_o is the earth's main field.

In both the inward drift theory and increasing magnetic field theory for IPDP, the change in emission frequency is governed by the change in magnetic field. The connection between the two theories is shown by the total derivative

$$\frac{D\vec{B}}{Dt} = \frac{\partial \vec{B}}{\partial t} + (\vec{v} \cdot \nabla)\ \vec{B} \qquad (6)$$

A moving particle sees the field change $\frac{D\vec{B}}{Dt}$ and it is this quantity which determines the change in frequency. In the increasing magnetic field theory the particles are assumed to remain at a fixed radial distance from the earth so $(\vec{v} \cdot \nabla)\vec{B} = 0$. Then $\frac{D\vec{B}}{Dt} = \frac{\partial \vec{B}}{\partial t}$ which is measured by the satellite after corrections for its motion. The close correspondence of f versus B, as measured by ATS-1, with time as the parameter and curves of constant $NW_{\parallel}$ (Fig. 23) means that $\frac{D\omega}{Dt}$ is determined by $\frac{\partial B}{\partial t}$ i.e. $|\frac{\partial \vec{B}}{\partial t}| > |(\vec{v} \cdot \Delta)\vec{B}|$ for the resonating protons.

The term $(\vec{v} \cdot \nabla \vec{B})$ may be non-zero, however, due to the existence of the changing magnetic field. That is, the magnetohydrodynamic (MHD) equation

$$\frac{\partial \vec{B}}{\partial t} = \nabla \times \vec{v} \times \vec{B} \qquad (7)$$

says that a changing magnetic field will produce internal plasma motions. To find the exact form of $\vec{v}$, the whole set of MHD equations would have to be solved throughout the region where $\frac{\partial \vec{B}}{\partial t} \neq 0$.

It is possible to make a rough magnitude calculation for $(\vec{v} \cdot \nabla)\vec{B}$ if an idealized model is used. For this calculation it is assumed:

1) that $\frac{\partial \vec{B}}{\partial t}$ is constant in the magnetospheric sector bounded by an angle ϕ_o and radial distance R (see Fig. 25),

2) that $\vec{E}$ (electric field) is not a function of ϕ .

Assumption (1) is reasonable since in the dusk-midnight sector almost the same $\frac{\partial \vec{B}}{\partial t}$ is recorded at ATS-1 satellite and directly below it at Honolulu (Cummings et al. 1968). Assumption (2) is not completely valid since it means that the electric field is circularly symmetric while the $\frac{\partial \vec{B}}{\partial t}$ change which produces the $\vec{E}$ field is confined to the dusk-midnight sector. This model therefore will produce only an upper limit for $(\vec{v} \cdot \nabla)\vec{B}$.

The electric field can be evaluated from the Maxwell equation in integral form.

$$\oint_c \vec{E} \cdot d\vec{l} = - \frac{\partial}{\partial t} \int_s \vec{B} \cdot d\vec{a}$$

where c and s are the contour and surface of the sector in Fig. 25. The contribution from AB and CA to $\vec{E} \cdot d\vec{l}$ will cancel so

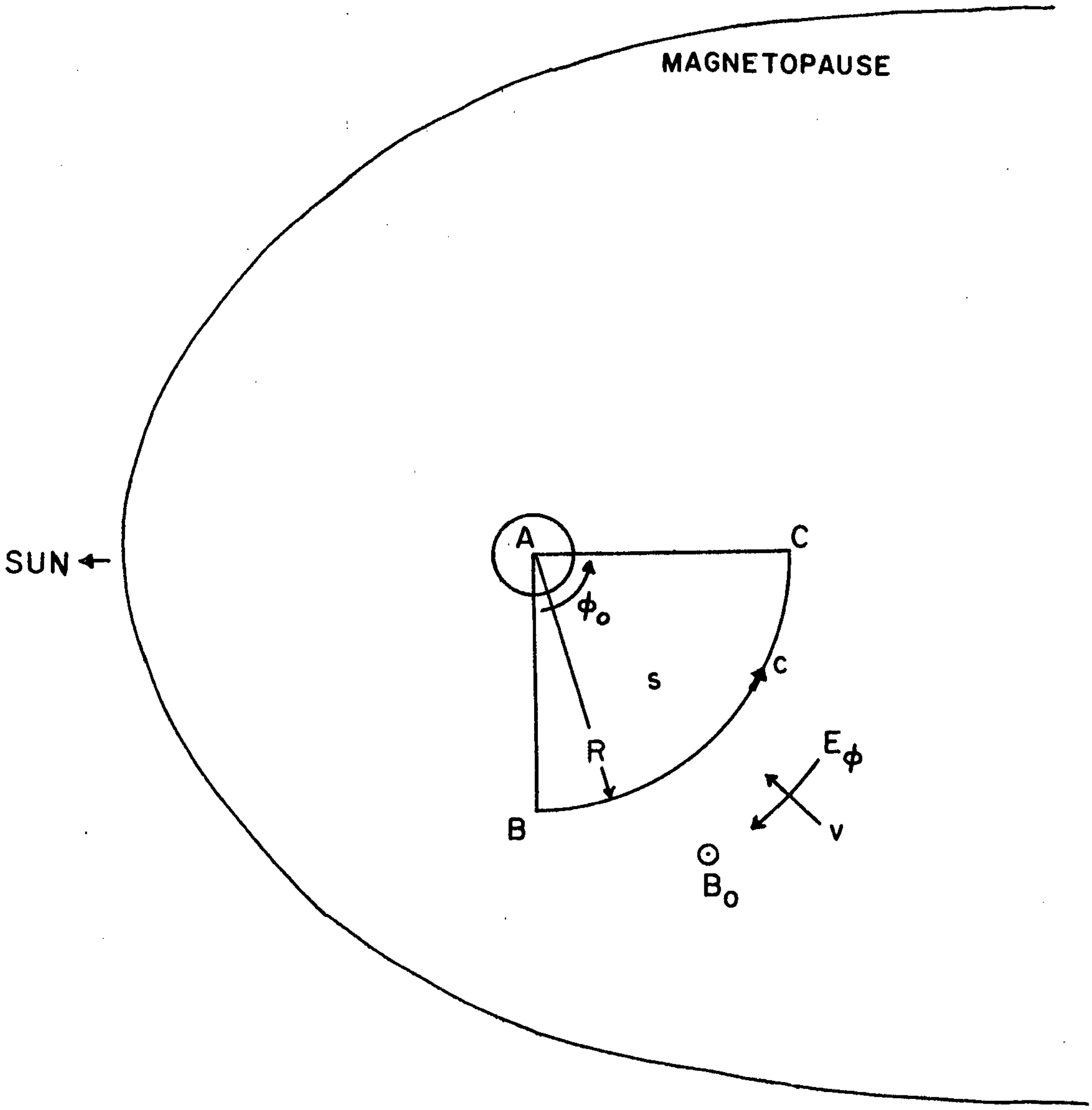

Fig. 25. Integration contour (c) and surface area (s) for calculation of electric field

$$E_\phi R \phi_o = - \frac{\partial}{\partial t} B \frac{R^2 \phi_o}{2}$$

$$\text{or} \qquad E_\phi = - \frac{1}{2} R \frac{\partial B}{\partial t}$$

An electric field in the minus ϕ direction will cause the plasma to drift inward at a speed $v = E/B$. The field B is taken as the earth's dipole field, i.e. the ring current field is ignored. Under these conditions:

$$|(\vec{v}\cdot\nabla)\vec{B}| = - v \frac{\partial B}{\partial R}$$

$$= 3/2 \frac{\partial B}{\partial t}$$

The upper limit of $(\vec{v}\cdot\nabla)\vec{B}$ is of the same order of magnitude as $\frac{\partial \vec{B}}{\partial t}$ but the actual value of $(\vec{v}\cdot\nabla)\vec{B}$ may be much smaller. The frequency increase of an IPDP due to inward drift is, in the extreme case, only comparable to the frequency increase due to $\frac{\partial \vec{B}}{\partial t}$.

The inward diffusion theory takes the opposite approach. In it $\frac{\partial \vec{B}}{\partial t}$ is assumed equal to zero. But to evaluate the theory it is also necessary to assume that the diffusion process does not affect the background plasma. This is necessary since (from (7)) motion of the background plasma will produce a $\frac{\partial \vec{B}}{\partial t}$ which cannot be calculated easily.

Using these assumptions, the change in magnetic field seen by the diffusing particle is

$$\frac{D\vec{B}}{Dt} = (\vec{v}_d \cdot \nabla)\vec{B} \tag{8}$$

The diffusion velocity $\vec{v}_d$ can be considered contained in the equatorial plane and directed inward. The magnetic field is the earth's dipole field ($B = \frac{B_{eq}}{R^3}$, where R is the distance to IPDP generation region).

The amount of inward diffusion necessary to explain IPDP's can now easily be found from (8)

$$\frac{DB}{Dt} = - v_d \frac{\partial B}{\partial R}$$

$$= \frac{3\, v_d\, B}{R}$$

and from (5)

$$\frac{D\omega}{Dt} = \frac{3}{2}\,\frac{\omega}{B}\,\frac{DB}{Dt}$$

$$= \frac{9}{2}\,\frac{\omega\, v_d}{R}$$

$$\text{so} \quad v_d = \frac{2}{9}\,\frac{R}{\omega}\,\frac{D\omega}{Dt} \tag{9}$$

The amount of inward diffusion is determined by measuring ω and $\frac{D\omega}{Dt}$ from the sonagrams and using the distance to IPDP generation region for R . The results of this analysis for several Ralston IPDP's is shown in table V.1. The average diffusion velocity of the events shown is 6.1 x 10^3 m/sec. A value of 6 Re for R has been used and if this is increased to 8 Re, the average diffusion velocity becomes 8.1 x 10^3 m/sec.

Lacourly (1969) attributes this inward diffusion to an electric field $\vec{E}$, producing a drift

$$\vec{v} = \frac{\vec{E} \times \vec{B}}{B^2}$$

However, the cold background plasma will also drift at the same velocity so the set of MHD equations would have to be solved before $\frac{D\vec{B}}{Dt}$ and thus $\frac{D\omega}{Dt}$ could be determined. Ignoring this effect Lacourly estimates an electric field of about 5 x 10^{-4} volts/m. The equivalent electric field for the average drift velocity determined above is $|E| = |B\ v_d| = 8.8 \times 10^{-4}$ volts/meter.

The main criticism of the inward diffusion theory is that no diffusion velocities or azimuthal electric fields of the above magnitudes have been measured in the dusk region of the magnetosphere. Also the main assumption that $\frac{\partial B}{\partial t} = 0$ has been proven invalid by ATS-1 measurements.

Fukunishi (1969) explains the IPDP frequency rise not by a changing magnetic field but by a decrease in energy of the

Table V.1

Inward Drift Velocities and Electric Field Necessary for Explanation of IPDP

Date	Local Time	$\frac{df}{dt}$ hertz/sec x 10^4	f hertz	Vd m/sec x 10^3	E volts/m x 10^{-4}
Jan. 21	22:30	2.7	0.62	3.7	5.3
March 18	22:40	1.0	0.37	2.3	3.3
March 27	18:50	1.1	0.18	5.2	7.4
April 17	19:50	4.7	0.54	7.4	10.5
May 7	21:20	4.2	0.70	5.1	7.3
May 16	22:20	3.7	0.45	7.0	10.0
May 17	22:00	1.6	0.58	2.3	3.3
Aug. 14	19:50	4.0	0.27	13.0	18.5
Sept. 13	22:40	0.5	0.14	3.0	4.3
Nov. 2	13:40	5.5	0.40	12.0	17.0
			Average	6.1	8.8

resonating protons. The protons are assumed to be impulsively injected into the nighttime magnetosphere at the start of a substorm expansion. Due to the gradient and curvature of the magnetic field the protons drift westward at the speed

$$v = \frac{c}{e} \nabla_{\perp} B \; (W_{\perp} \div 2W_{\parallel})$$

Since this velocity varies directly with the proton energy, an observer at a fixed longitude would see a gradually softening proton beam. If the protons have a suitable velocity distribution for cyclotron instability wave amplification an IPDP will be produced $(\omega \propto 1/\sqrt{W_{\parallel}})$.

Fukunishi does not take into account the changing magnetic field in the dusk-midnight sector of the magnetosphere. His calculation of proton drift velocities is thus for a steady state magnetosphere, which is a poor approximation during magnetospheric substorms.

The differential drift theory can not easily explain the intimate relationship between IPDP's, 4-sec. micropulsations and hm emissions. Fukunishi uses stably trapped protons for 4-sec. micropulsation generation and transiently trapped protons for IPDP generation. It is much simpler to consider a single particle source with a static and then changing magnetic field producing the difference between the two types of micropulsations.

CHAPTER VI

Discussion of Future Experiments

The increasing magnetic field theory for IPDP relates the frequency change of IPDP noise band to the change in the ion cyclotron instability frequency due to an increasing magnetic field. Hm emissions and band type micropulsations (4-sec. period micropulsations) are also generated by a cyclotron instability process, and the relationship between these three types of micropulsations has been discussed briefly in Section V.1. In order to firmly establish the ideas presented there, further experimental and theoretical work needs to be done. In particular, the characteristics of band type emissions must be more extensively studied. One of the main problems is to establish the similarities and differences in the structural elements in hm emissions, IPDP's and band type micropulsations. A conjugate pair of stations would be necessary for this purpose.

Since there is a direct relationship between IPDP's and magnetospheric substorms, IPDP's might provide valuable information on the substorm process. The increasing magnetic field theory relates the IPDP frequency change to a magnetic field change associated with a partial ring current in the dusk-midnight quadrant of the magnetosphere. Thus IPDP's can be used to help deduce the form of the three dimensional current system existing during magnetospheric substorms. More specifically, IPDP's are generated at the time of removal of this partial ring current which likely corresponds to the formation of the auroral bulge and westward travelling surge. A careful study of IPDP properties could lead to a better understanding of the complex dynamic processes occurring during magnetospheric substorms.

To achieve the aims given above, multi-station micropulsation experiments must be performed. A line of micropulsation stations at approximately the same geomagnetic latitude could determine: 1) the longitudinal extent of individual IPDP's 2) IPDP frequency versus longitude (L.T.) for individual events and 3) the simultaneity of the same IPDP observed at different longitudes. A line of stations at the same geomagnetic longitude could determine 1) the field line on which the IPDP was generated and 2) IPDP frequency characteristics versus latitude. IPDP studies of this type would provide information which could be related to the magnetospheric substorm process.

Data from a network of micropulsation stations would also further establish (or disprove) the increasing magnetic field theory. The increasing magnetic field theory predicts a relatively static region of IPDP generation whereas the inward diffusion theory predicts an inward motion of this region. The motion, or lack of it, might be established by detecting a change in latitude of maximum IPDP energy. However, this difference would be difficult to establish due to a number of unknowns (ionospheric absorption, duct propagation, crustal conductivity, etc.). The differential drift theory predicts a time delay for an IPDP observed in the dusk region relative to time of the same IPDP nearer midnight. The lack of a time delay would disprove that theory.

BIBLIOGRAPHY

Akasofu, S. I., The development of the auroral substorm, Planet. Space Sci., 12, 273, 1964.

Akasofu, S. I., Polar and magnetospheric substorms, D. Deidel Publishing Co., Dordrecht, Holland, 1968.

Akasofu, S. I., and C. I. Meng, Intense bays inside the auroral zone. I. The evening sector, J. Atmospheric Terrest. Phys., 29, 965, 1967.

Akasofu, S. I., and C. I. Meng, A study of polar magnetic substorms, J. Geophys. Res., 74, 293, 1969.

Akasofu, S. I., S. Chapman, and C. I. Meng, Dynamics of the aurora II Westward travelling surges, J. Atmospheric Terrest. Phys., 27, 173, 1965a.

Akasofu, S. I., S. Chapman, and C. I. Meng, The polar electrojet, J. Atmospheric Terrest. Phys., 27, 1275, 1965b.

Akasofu, S. I., C. I. Meng, and D. S. Kimball, Dynamics of the aurora IV, Polar magnetic substorms and westward travelling surges, J. Atmospheric Terrest. Phys., 28, 489, 1966a.

Akasofu, S. I., D. S. Kimball, and C. I. Meng, Dynamics of the aurora V. Poleward Motions, J. Atmospheric Terrest. Phys., 28, 497, 1966b.

Anderson, K. A., Energetic electron fluxes in the tail of the geomagnetic field, J. Geophys. Res., 70, 4741, 1965.

Angenheister, G., Uber die Fortpflanzungs-Geschwindigkeit Magnetischer Storungen und Pulsationen, Bericht uber die Erdmagnetischen Cheltenham, and Tsingtau in September 1911, Gott, Nach. Ges. Wiss., 565, 1912.

Astrom, E., On waves in ionized gas, Ark. Fys., 2, 443, 1950.

Atkinson, G., The current system of geomagnetic bays, J. Geophys. Res., 72, 6063, 1967.

Barry, J. D., and R. C. Snare, A fluxgate magnetometer for the Applications Technology Satellite, IEEE Trans. Nuclear Sci., NS-13, 1966.

Behannon, K. W., and N. F. Ness, Magnetic storms in the earth's magnetic tail, J. Geophys. Res., 71, 2327, 1966.

Best, A., G. Fanselau, A. Grafe, H. E. Schmau, Chr.-Ulr. Wagner, The variations of the geomagnetic field in middle and high latitudes during the quiet period from June 28th to July 18th 1966, Rept. 301, Geomagnet. Inst., German Academy of Sciences, Berlin, Potsdam, 1968.

Brown, W. L., L. J. Cahill, L. R. Davis, C. E. McIlwain, and C. S. Roberts, Acceleration of trapped particles during a magnetic storm on April 18, 1965, J. Geophys. Res., 73, 153, 1968.

Carpenter, D. L., Whistler studies of the plasmapause in the magnetosphere 1., J. Geophys. Res., 71, 693, 1966.

Cornwall, J. M., Cyclotron instabilities and electromagnetic emission in the ultra low frequency and very low frequency ranges, J. Geophys. Res., 70, 61, 1965.

Coroniti, F. V., R. L. McPherron, G. K. Parks, Studies of magnetospheric substorm, 3, J. Geophys. Res., 73, 1715, 1968.

Cummings, W. D., and P. J. Coleman, Jr., Simultaneous magnetic field variations at the earth's surface and at synchronous equatorial distance, 1, Bay-associated events, Radio Sci., 3, 758, 1968.

Cummings, W. D., J. N. Barfield, and P. J. Coleman, Jr., Magnetospheric substorms observed at the synchronous orbit, J. Geophys. Res., 73, 6687, 1968.

Dowden, R. L., and M. W. Emergy, The use of micropulsation whistlers in the study of the outer magnetosphere, Planet. Space Sci., 13, 773, 1965.

Duffus, H. J., P. W. Nasmyth, J. A. Shand, and C. Wright, Subaudible geomagnetic fluctuations, Nature, 181, 1258, 1959.

Feldstein, Y. I., Auroral morphology, 1 and 2, Tellus, 16, 252, 1964.

Feldstein, Y. I., Peculiarities in the auroral distribution and magnetic disturbance distribution in high latitudes caused by the asymmetrical form of the magnetosphere, Planet. Space Sci., 14, 121, 1966.

Fukunishi, H., Occurrence of sweepers in the evening sector following the onset of magnetospheric substorms, Rep. Ionos. Space Res. Japan, 23, 21, 1969.

Gendrin, R., Gyroresonance radiation produced by proton and electron beams in different regions of the magnetosphere, J. Geophys. Res., 70, 5369, 1965.

Gendrin, R., M. Gokhberg, S. Lacourly and V. A. Troitskaya, Apparition simultanée de pulsations magnétiques d'ultrabasse fréquence en phase en deux points conjugués, C. R. Acad. Sc. Paris, 262, 845, 1966.

Gendrin, R., S. Lacourly, V. A. Troitskaya, M. Gokhberg, and R. V. Shepetnov, Caractéristiques des pulsations irrégulières de période décroissante (IPDP) et leurs relations avec les variations du flux des particules piégées dans la magnétosphère, Planet. Space. Sci., 15, 1239, 1967.

Gibb, C. A., An assessment of slow speed tape recorder system, Defense Research Establishment Pacific, Technical Memorandum 68-8, 1968.

Greifinger, C., and P. S. Greifinger, Theory of hydromagnetic propagation in the ionospheric waveguide, J. Geophys. Res., 73, 7473, 1968.

Heacock, R. R., The 4-second summertime micropulsation band at College, J. Geophys. Res., 71, 2763, 1966.

Heacock, R. R., Evening micropulsation events with a rising midfrequency characteristic, J. Geophys. Res., 72, 399, 1967a.

Heacock, R. R., Two subtypes of type Pi micropulsations, J. Geophys. Res., 72, 3905, 1967b.

Heacock, R. R., and V. P. Hessler, Pearl-type micropulsations associated with magnetic storm sudden commencements, J. Geophys. Res., 70, 1103, 1965.

Jacks, B., The origin of hydromagnetic emissions, Earth Planet. Sci. Letters, 1, 467, 1966.

Jacks, B., The exact theory of linear cyclotron instabilities applied to hydromagnetic emissions in the magnetosphere, M.Sc. thesis, University of British Columbia, 1966.

Jacobs, J. A. and T. Watanabe, Micropulsation whistlers, J. Atmospheric Terrest. Phys., 26, 825, 1964a.

Jacobs, J. A. and T. Watanabe, Symp. Ultra Low Frequency Electromagnetic Fields, Boulder, Colorado, 1964b.

Jacobs, J. A. and T. Watanabe, Amplification of hydromagnetic waves in the magnetosphere by a cyclotron instability process with applications to the theory of hydromagnetic whistlers, Boeing Scientific Research Laboratories Report 01-82-0398, 1965.

Jacobs, J. A. and T. Watanabe, Amplification of hydromagnetic waves in the magnetosphere by a cyclotron instability process with applications to the theory of hydromagnetic whistlers, J. Atmospheric Terrest. Phys., 28, 235, 1966.

Jacobs, J. A. and T. Watanabe, Theoretical notes on whistlers and periodic emissions in the hydromagnetic regime, Planet. Space Sci., 15, 799, 1967.

Jacobs, J. A., Y. Kato, S. Matsushita, and V. A. Troitskaya, Classification of geomagnetic micropulsations, J. Geophys. Res., 69, 180, 1964.

Jelley, D. H., and N. Brice, Association between increased radiation in the outer belt and polar auroral substorms, Trans. Am. Geophys. Union, 48, 180, 1967.

Knaflich, H. B., and J. F. Kenney, IPDP events and their generation in the magnetosphere, Earth Planet. Sci. Lett., 2, 453, 1967.

Knaflich, H. B., and J. F. Kenney, Longitudinal spread of Pc 1 micropulsations in the magnetosphere, Nature, 217, 1134, 1968.

Konradi, A., Proton events in the magnetosphere associated with magnetic bays, J. Geophys. Res., 72, 3829, 1967.

Konradi, A., Rapid increases in the proton and electron fluxes in the magnetosphere, J. Geophys. Res., 73, 3449, 1968.

Lacourly, S., Évaluation de certains paramètres de la magnétosphère à partir des propriétés des pulsations hydromagnétiques irrégulières (SIP et IPDP), Ann. Geophys., 25, 651, 1969.

Liemohn, H. B., Cyclotron-resonance amplification of VLF and ULF whistlers, J. Geophys. Res., 72, 39, 1967.

Lokhen, J. E., Natural Electromagnetic Phenomena Below 30Kc/s., Plenum Press, New York, 1964.

Manchester, R. N., Propagation of Pc 1 micropulsations from high to low latitudes, J. Geophys. Res., 71, 3749, 1966.

McPherron, R. L., G. K. Parks and F. V. Coroniti, Relation of correlated magnetic micropulsations and electron precipitation to the auroral substorm, Conjugate Point Symposium, June 1967, Boulder, Colorado, p III-4-1, 15, ITSA Mem., 72, July, 1967.

McPherron, R. L., G. K. Parks, F. V. Coroniti, and S. H. Ward, Studies of the magnetospheric substorm 2. Correlated magnetic micropulsations and electron precipitation occurring during auroral substorms, J. Geophys. Res., 73, 1697, 1968.

Mead, G. D., Deformation of the geomagnetic field by the solar wind, J. Geophys. Res., 69, 1181, 1964.

Meng, C. I. and S. I. Akasofu, A study of polar magnetic substorms, 2. Three dimensional current system, J. Geophys. Res., 74, 4035, 1969.

Obayashi, T., Symp. Ultra low frequency electromagnetic fields, Boulder, Colorado, 1964.

Obayashi, T., Hydromagnetic whistlers, J. Geophys. Res., 70, 1069, 1965.

Rostoker, G., The characteristics and world-wide propagation of Pi 2 micropulsations, Ph.D. thesis, University of British Columbia, 1966.

Rostoker, G., Macrostructure of geomagnetic bays, J. Geophys. Res., 73, 4217, 1968.

Selsbee, H. C. and E. H. Vestine, Geomagnetic bays, their frequency and current systems, Terrest. Magnet. Atmospheric Elec., 47, 195, 1942.

Sobouti, Y., The relationship between unique geomagnetic and auroral events, J. Geophys. Res., 66, 725, 1961.

Tepley, L. R., A study of hydromagnetic emissions, Sci. Rept. 2 (contract AF 19(604)-5906, Electron. Res. Directorate, Air Res. Devel. Command), April 14, 1961.

Tepley, L. R., Structure and attenuation of hydromagnetic emissions, Vol. 1, Sci. Rept. 1 (contract AF 19(604)-5906, Electron. Res. Directorate, Air Res. Devel. Command), April 6, 1962.

Tepley, L. R., Recent investigations of hydromagnetic emissions. Part I. Experimental observations, J. Geomag. Geoelect., 18, 227, 1966.

Tepley, L. R. and K. D. Amundsen, Notes on sub ELF emissions observed during magnetic storms, J. Geophys. Res., 69, 3749, 1964.

Tepley, L. R. and R. C. Wentworth, Hydromagnetic emissions, X-ray bursts, and electron bunches, 1. Experimental results, J. Geophys. Res., 67, 3317, 1962.

Tepley, L. R. and R. K. Landshoff, Waveguide theory for ionospheric propagation of hydromagnetic emissions, J. Geophys. Res., 71, 1499, 1966.

Tereda, T., On rapid periodic variations of terrestrial magnetism, Journal of the College of Science, Imperial University of Tokyo, May 25th, XXVII, Art. 9. de Moidrey, S.J.: Pulsations magnétiques à Zi-Ka-Wei et à Lu-kiv-pang, Terr. Mag., 22, 113, 1917.

Troitskaya, V. A., Pulsations of the earth's electromagnetic field with periods of 1 to 15 seconds and their connection with phenomena in the high atmosphere, J. Geophys. Res., 66, 5, 1961.

Troitskaya, V. A., and N. F. Mal'tseva, Possible influence of ionospheric conditions on the formation of pulsations on intervals of decreasing period in the electromagnetic field of the earth, Geomag. Aerom., 6, 915, 1967.

Watanabe, T., Determination of the electron distribution in the magnetosphere using hydromagnetic whistlers, J. Geophys. Res., 70, 5839, 1965.

Weir, R. C., An FM slow-speed tape recorder system, Pacific Naval Laboratory Technical Memorandum 66-2, 1966.

Williams, D. J. and G. D. Mead, Nightside magnetosphere configurations as obtained from trapped electrons at 1000 kilometers, J. Geophys. Res., 70, 3017, 1965.

Zmuda, A. J., J. H. Martin, and F. T. Heuring, Transverse magnetic disturbance at 1100 km in the auroral region, J. Geophys. Res., 71, 5033, 1966.

APPENDIX I

SPECIFICATIONS OF KAY ELECTRIC SONAGRAPH 7030A

FREQUENCY RANGE: 1 to 16000 Hz in eight ranges

Range (Hz)	Record Time (sec.)	Resolution (Hz)
1 - 100	192.5	0.56 & 3.8
4 - 400	48.1	2.2 & 15.2
5 - 500	38.4	2.8 & 19.0
10 - 1000	19.2	5.6 & 37.5
20 - 2000	9.6	11.2 & 75
40 - 4000	4.8	22.5 & 150
80 - 8000	2.4	45 & 300
160 - 16000	1.2	90 & 600

RESPONSE: ± 2db over entire range

AGC RANGE: Variable 20 to 40 down to 10db

AMPLIFIER CHARACTERISTICS: Flat or 13db high shape

INPUT IMPEDANCE: 200, 600, or 10,000 ohms switchable

ANALYSIS TIME: 1.3 min.

DISPLAYS AVAILABLE: Frequency-vs-amplitude-vs-time (conventional and contour)

Amplitude-vs-frequency

Amplitude-vs-time

APPENDIX II

ION CYCLOTRON INSTABILITY FREQUENCY VERSUS MAGNETIC FIELD

The dispersion equation for a left-handed ion cyclotron wave propagating parallel to the background magnetic field is:

$$\omega^2 - c^2k^2 - \sum_{comp} \frac{\Omega_p^2 \omega}{\omega - \Omega} = 0 \qquad (1)$$

where $\Omega_p^2 = \frac{4\pi N e^2}{m}$, $\Omega = \frac{qB_o}{mc}$

For a plasma consisting of protons and electrons

$$\omega^2 - c^2k^2 - \frac{\Omega_{pi}^2 \omega}{\omega - \Omega_i} - \frac{\Omega_{pe}^2 \omega}{\omega - \Omega_e} = 0 \qquad (2)$$

Using the approximations:

$$m_e << m_i$$

$$\omega << \Omega_e$$

equation (2) becomes on algebraic manipulation:

$$\omega^2 - c^2k^2 - \frac{4\pi N_i e \omega^2 c}{B_o(\omega - \Omega_i)} = 0 \qquad (3)$$

the resonance condition for streaming protons

$$\omega - ku - \Omega_i = 0 \tag{4}$$

is substituted into (3) and using the approximation that the streaming velocity $u << c$ we get:

$$N_i W_{\parallel} = \frac{e^2}{8\pi m_i^2 c^2}\left(1 - \frac{\omega}{\Omega_i}\right)^3 \frac{B_o^4}{\omega^2}$$

where:

N_i - background plasma density

B_o - background magnetic field

$W_{\parallel}$ - parallel energy of streaming protons

APPENDIX III

USE OF ION CYCLOTRON DISPERSION EQUATION WITH A CHANGING B FIELD

The frequency of an ion cyclotron instability has been determined in Appendix II using the dispersion equation for ion cyclotron waves with a constant background field. The instability frequency is then considered to change due to a changing background magnetic field. This procedure is valid due to the large difference in time scales of phenomena.

$$T_\omega << T_g << T_e \qquad (1)$$

$T_\omega \sim 1$ sec	period for ion rotation about magnetic field line equal to doppler shifted wave period
$T_g \sim 100$ sec	growth time for ion cyclotron instabilities
$T_e \sim 2 \times 10^3$ sec	time duration of IPDP

The validity of inequality (1) assures that B is approximately constant over

1) many cycles of the wave necessary for the growth of the cyclotron instability

2) the time required to establish a frequency from the sonagram for a comparison with ATS-1 data.

APPENDIX IV

DEFINITION OF MAGNETIC COMPONENTS

The earth's magnetic field at any point can be represented by a vector which is described by its magnitude and direction relative to a selected co-ordinate system. Figure 26 illustrates seven magnetic elements (X, Y, Z, H, D, I, F) often used in describing the magnetic field.

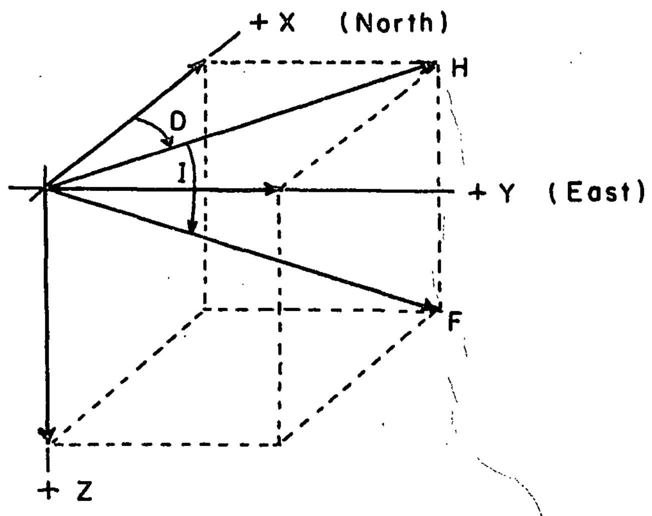

Fig. 26. Graphic representation of the elements of a magnetic vector: X, Y, Z (geographic north, east, and vertical components), H (horizontal intensity), D (declination), I (inclination), and F (total intensity).

Surface observatories commonly measure either H, D, and Z or X, Y, Z using variometers plus an absolute measurement to establish the baseline. In this procedure D is measured as a magnetic field change perpendicular to H direction. It can be expressed thus either as a magnetic field change or converted into an angle change in declination.